NeuroImage 207 (2020) 116391

Contents lists available at ScienceDirect

NeuroImage

journal homepage: www.elsevier.com/locate/neuroimage

Music enhances structural maturation of emotional processing neural pathways in very preterm infants

Joana Sa de Almeida [a], Lara Lordier [a], Benjamin Zollinger [b], Nicolas Kunz [c], Matteo Bastiani [d,e,f], Laura Gui [g], Alexandra Adam-Darque [a], Cristina Borradori-Tolsa [a], François Lazeyras [g], Petra S. Hüppi [a,*]

[a] Division of Development and Growth, Department of Woman, Child and Adolescent, University Hospitals of Geneva, Geneva, Switzerland
[b] Department of Psychology of Yale University, New Haven, CT, USA
[c] Center of BioMedical Imaging (CIBM), Ecole Polytechnique Fédérale de Lausanne (EPFL), Lausanne, Switzerland
[d] Sir Peter Mansfield Imaging Centre, School of Medicine, University of Nottingham, UK
[e] NIHR Biomedical Research Centre, University of Nottingham, UK
[f] Wellcome Centre for Integrative Neuroimaging (WIN) - Centre for Functional Magnetic Resonance Imaging of the Brain (FMRIB), University of Oxford, UK
[g] Department of Radiology and Medical Informatics, Center of BioMedical Imaging (CIBM), University of Geneva, Geneva, Switzerland

ARTICLE INFO

Keywords:
Diffusion tensor imaging
Emotional processing
Human brain development
Music intervention
Preterm birth

ABSTRACT

Prematurity disrupts brain maturation by exposing the developing brain to different noxious stimuli present in the neonatal intensive care unit (NICU) and depriving it from meaningful sensory inputs during a critical period of brain development, leading to later neurodevelopmental impairments.

Musicotherapy in the NICU environment has been proposed to promote sensory stimulation, relevant for activity-dependent brain plasticity, but its impact on brain structural maturation is unknown. Neuroimaging studies have demonstrated that music listening triggers neural substrates implied in socio-emotional processing and, thus, it might influence networks formed early in development and known to be affected by prematurity.

Using multi-modal MRI, we aimed to evaluate the impact of a specially composed music intervention during NICU stay on preterm infant's brain structure maturation. 30 preterm newborns (out of which 15 were exposed to music during NICU stay and 15 without music intervention) and 15 full-term newborns underwent an MRI examination at term-equivalent age, comprising diffusion tensor imaging (DTI), used to evaluate white matter maturation using both region-of-interest and seed-based tractography approaches, as well as a T2-weighted image, used to perform amygdala volumetric analysis.

Overall, WM microstructural maturity measured through DTI metrics was reduced in preterm infants receiving the standard-of-care in comparison to full-term newborns, whereas preterm infants exposed to the music intervention demonstrated significantly improved white matter maturation in acoustic radiations, external capsule/claustrum/extreme capsule and uncinate fasciculus, as well as larger amygdala volumes, in comparison to preterm infants with standard-of-care. These results suggest a structural maturational effect of the proposed music intervention on premature infants' auditory and emotional processing neural pathways during a key period of brain development.

1. Introduction

Preterm birth, accounting for approximately 15 million yearly cases worldwide, is associated with a range of long-term complications (Blencowe et al., 2013), in particular neurodevelopmental disorders. Such complications stem from the fact that preterm birth disrupts the normal brain maturation during a critical period of fetal brain growth (Brody et al., 1987; Dubois et al., 2008; Huang et al., 2006; Kiss et al., 2014; Nossin-Manor et al., 2013; Volpe, 2009), exposing the developing brain to different noxious events in the neonatal intensive care unit (NICU) and depriving it from meaningful sensory inputs relevant for activity-dependent plasticity (Kiss et al., 2014; Radley and Morrison,

* Corresponding author. Hôpitaux Universitaires de Genève; Département de la femme, de l'enfant et de l'adolescent, Service de développement et croissance, Hôpital des enfants, Rue Willy-Donzé 6, CH-1211, Genève 14, Switzerland.
E-mail address: petra.huppi@hcuge.ch (P.S. Hüppi).

https://doi.org/10.1016/j.neuroimage.2019.116391
Received 25 July 2019; Received in revised form 18 November 2019; Accepted 21 November 2019
Available online 22 November 2019

2005).

Although advances in neonatal medicine have improved preterm infants' outcome, dedicated brain-oriented care has not been established yet (Als and McAnulty, 2014; Chang, 2015; Sizun and Westrup, 2004). Up to 40%–50% of very preterm infants (VPT), those born before 32 weeks gestational age (GA), still experience neurodevelopmental impairments evident in childhood (Anderson and Doyle, 2003; Bhutta et al., 2002; Marlow, 2004; Montagna and Nosarti, 2016; Spittle et al., 2009, 2011; Williams et al., 2010; Witt et al., 2014), and 25% of VPT infants evidence behavioral impairments, characterized by inattention, anxiety, internalizing and socio-emotional problems (Anderson and Doyle, 2003; Arpi and Ferrari, 2013; Bhutta et al., 2002; Marlow, 2004; Montagna and Nosarti, 2016; Spittle et al., 2009, 2011; Williams et al., 2010; Witt et al., 2014). Moreover, VPT infants are at higher risk of developing psychiatric disorders, such as attention deficit and hyperactivity disorder (ADHD), autism spectrum disorder (ASD), anxiety and depression (Johnson and Marlow, 2011; Nosarti et al., 2012; Treyvaud et al., 2013).

By term-equivalent age (TEA) and also later in childhood and adulthood, the preterm brain has been found to be structurally different from that of a healthy full-term born individual. Magnetic resonance imaging (MRI) has evidenced early developmental brain anomalies in preterm infants, such as regional cortical and subcortical volumes changes (Ball et al., 2017; Cismaru et al., 2016; Huppi and Dubois, 2006; Ment et al., 2009; Nosarti, 2013; Padilla et al., 2015; Peterson et al., 2000) and alterations of brain networks and their microstructural characteristics (Fischi-Gomez et al., 2015; Pecheva et al., 2018; Rogers et al., 2012), which were shown to correlate with specific neuropsychological deficits after preterm birth. In particular, preterm infants were found to present structural brain alterations in regions thought to subserve emotional processing and which were related to later socio-emotional deficits. These alterations include reduced volumes of amygdala, hippocampus, orbito-frontal cortex (OFC), insula and posterior cingulate cortex (Aanes et al., 2015; Anjari et al., 2007; Ball et al., 2012; Cismaru et al., 2016; Gimenez et al., 2006; Huppi et al., 1998; Inder et al., 2005; Nosarti et al., 2014; Peterson et al., 2000; Rogers et al., 2012; Thompson et al., 2007, 2013), white matter (WM) immaturity of the OFC regions (Rogers et al., 2012), prefrontal and medial orbito-frontal-cortico-striatal networks (Fischi-Gomez et al., 2016), and of several WM tracts, namely forceps minor, forceps major, inferior fronto-occipital fasciculus/inferior longitudinal fasciculus, superior longitudinal fasciculus and external capsule (Loe et al., 2013; Skranes et al., 2007).

Recently, NICUs have been searching for developmentally oriented care to modulate preterm infants' sensory input during this critical period of development, with the aim of improving early brain maturation. Music has been an implemented approach for meaningful sensory stimulation during NICU stay, thought to be relevant for activity-dependent brain plasticity during a critical period of auditory maturation (Graven and Browne, 2008; Kiss et al., 2014; Lasky and Williams, 2005). In adults, music listening is known to trigger neural substrates involved in socio-emotional functions, comprising amygdala, hippocampal formation, ventral striatum (including nucleus accumbens), pre-supplementary motor area, cingulate cortex, insula and OFC (Koelsch et al., 2004; Koelsch, 2010; Popescu et al., 2004; Zatorre et al., 2009). Thus, music listening might hold the potential to modulate neural networks known to be affected by prematurity early in development and in particular involved in socio-emotional processing.

However, to date, there is little evidence of the effect of music on preterm infants' brain development. An ultrasound study has shown that the enrichment of preterm infants' early postnatal environment with audio recordings of maternal sounds (heartbeat, speech, reading and singing voice) increases cortical thickness in the primary auditory cortex (Webb et al., 2015). In a fMRI study, preterm infants exposed to a specific music intervention during NICU stay, when at term-age, had an increased functional connectivity between the primary auditory cortex and the thalamus, middle cingulate cortex and striatum when listening to the known music, regions linked to familiarity, pleasant and arousing music processing (Lordier et al., 2019a). Additionally, the effect of this music intervention was explored by means of its impact on preterm infants' resting-state functional connectivity. When compared to full-term infants, premature infants in the control group evidenced a decreased functional connectivity of the salience network (comprising bilateral insula and anterior cingulate) with other networks involved both in sensory and high level cognitive networks (auditory, sensorimotor, superior frontal, thalamus and precuneus networks). Conversely, preterm infants receiving the music intervention evidenced a higher functional connectivity in these same regions when compared to preterm infants control (Lordier et al., 2019b). However, the extent to which music listening during the early postnatal period in preterm infants can influence brain macrostructure and microstructural network maturation remains to be explored and is the primary aim of this study.

Diffusion tensor imaging (DTI) is a non-invasive MRI method that uses the diffusion anisotropy of water molecules within the tissues to allow *in vivo* visualization and quantification of WM microstructure and connectivity (Huppi and Dubois, 2006; Pierpaoli and Basser, 1996). It characterises water diffusion using a mathematical tensor model, allowing the calculation of several DTI-derived scalar indices, including: fractional anisotropy (FA), quantifying the degree of tissue anisotropy and which has been used to assess WM integrity (Kamagata et al., 2012; Kochunov et al., 2009; Onu et al., 2012); and mean diffusivity (MD) providing the overall magnitude of water diffusion. Rapid changes in FA and MD take place early in development: in preterm infants from 27 to 42 weeks GA, WM FA increases while the MD decreases (Aeby et al., 2009; Neil et al., 2002; Partridge et al., 2004), accompanying an increased WM-fiber organization, increased axonal density and coherence, decreased water content and preliminary myelination occurring during early brain development (Aeby et al., 2009; Beaulieu, 2002; Dubois et al., 2008; Mukherjee et al., 2002; Shim et al., 2012). To better characterize the mechanisms underlying FA modifications, studies investigate radial diffusivity (RD) and axial diffusivity (AD), indices also derived from the diffusion tensor. RD may be sensitive to myelination and correlates positively with mean axon diameter (Beaulieu, 2002), whereas AD alterations have been associated with axon morphologic changes, such as axonal density or calibre (Jones, 2011). Increased FA and decreased MD and RD in WM of preterm infants at TEA have been shown to be related to subsequent improved neurodevelopmental performance, namely motor, cognitive and language performance in early childhood (Counsell et al., 2008; Duerden et al., 2015; Krishnan et al., 2007), as well as improved visual function (Bassi et al., 2008; Groppo et al., 2014).

In this study, we used DTI to characterize the WM microstructural maturation in VPT infants exposed to music during NICU stay, in comparison to VPT infants receiving the standard-of-care and to full-term infants, all at term age. For that purpose, we used a template-based region-of-interest (ROI) analysis method comprising 20 WM ROI and subsequently a seed-based tractography analysis of three selected tracts involved in auditory or socio-emotional processing: acoustic radiations, interhemispheric temporal callosal fibers and uncinate fasciculus. Additionally, at a macrostructural level, we aimed to assess if a music intervention in VPT infants during NICU stay could have an impact on amygdala volume, given amygdala's central role in emotion modulation during music processing and evidence of its volumetric reduction in preterm infants at both TEA and in adulthood, according to previous studies (Cismaru et al., 2016; Peterson et al., 2000).

We hypothesize that an early postnatal music intervention, during NICU hospitalization, can improve preterm infants' macro and microstructural brain maturation, falling in line with the expected developmental trajectory, in particular in the cortico-limbic networks.

2. Materials and methods

2.1. Subjects

39 VPT infants (GA at birth <32 weeks) were recruited at the neonatal unit of the University Hospitals of Geneva (HUG), Switzerland, from 2013 to 2016, as part of a prospective randomized clinical trial entitled 'The effect of music on preterm infant's development' (NCT03689725), registered at register.clinicaltrials.gov. Out of these, 20 received a music intervention during NICU stay (PTM), whereas 19 did not listen to music and received the standard-of-care during NICU stay (PTC).

Additionally, 40 full-term (FT) infants were recruited at the maternity of HUG, from 2011 to 2016 as part of clinical trials studying the impact of prematurity on neonatal preterm brain development.

Research Ethics Committee approval was granted for the studies and written parental consent was obtained prior to infant's participation to the studies.

Six preterm infants were excluded from the study before the MRI due to: parental refusal (2 PTM, 1 PTC), transfer to another hospital (1 PTM) and insufficient number of music intervention sessions (less than 15 intervention sessions: 2 PTM).

All subjects underwent an MRI examination at TEA (37–42 weeks GA). Infants whose MRI protocol acquisition was incomplete, not comprising a T2-weighted image and DTI sequence, or that presented major focal brain lesions or major movement on MRI images were excluded from the analysis. The final sample of infants used for DTI analysis consisted of: 15 PTM (7 females/8 males, mean GA at birth: 28.58 ± 2.30 weeks, mean GA at MRI: 40.15 ± 0.61 weeks), 15 PTC (10 females/5 males, mean GA at birth: 28.30 ± 2.34 weeks, mean GA at MRI: 40.48 ± 0.61 weeks) and 15 FT infants (9 females/6 males, mean GA at birth: 39.32 ± 1.03 weeks, mean GA at MRI: 39.63 ± 1.02 weeks). The flow chart of the participant selection process is provided in Supplementary Fig. S1. No significant difference between the PTM and PTC groups was found in demographic and perinatal variables: GA at birth, weight, sex, height, head circumference at birth, neonatal asphyxia, bronchopulmonary dysplasia, intraventricular hemorrhages, sepsis (positive blood culture), GA at MRI and socio-economic parental status (Largo et al., 1989) (Table 1). Regarding T2-weighted images used for amygdala volumetric analysis, from the 45 infants retained for DTI analysis, 11 were excluded due to movement artifacts preventing correct amygdala segmentation. The remaining 34 infants included in this analysis were distributed as follow: 10 PTC, 11 PTM and 13 FT infants.

2.2. Music intervention

During NICU stay, from 33 weeks GA until discharge, the PTC group received standard-of-care, while the PTM group listened approximately five times per week (mean: 4.84 ± 1.18), through headphones, to an 8 min musical piece created for the project by the composer Andreas Vollenweider (http://vollenweider.com/en). The musical piece was selected among three different music tracks of 8 min duration, according to the waking state of the child (waking up, falling asleep, being active). All tracts were composed of sounds of harp, punji (charming snake flute) and bells, that interactively create a melody. The 8 min duration was chosen to suit the duration of the sleep-wake state transitions of the infant. The musical instruments and melody were chosen based on the behavioral and physiological responses of preterm newborns (for more details consult Appendix B of Lordier et al., 2019a).

2.3. MRI acquisition

All infants were scanned after receiving breast or formula feeding, during natural sleep and using a vacuum mattress for immobilization. No sedation was used. MR-compatible headphones were used (MR confon, Magdeburg, Germany) to protect infants from scanner's noise. All infants were monitored for heart rate and oxygen saturation during the entire scanning time.

Table 1
Clinical characteristics of the infants.

Clinical Characteristics	*Full-term* (FT) *n = 15*	*Preterm Music (PTM) n = 15*	*Preterm Control (PTC) n = 15*	*p-value*[a] *PTM vs PTC*
Gestational age at birth, weeks, mean (SD)	39.2 (±1.3)	28.58 (±2.3)	28.30 (±2.3)	0.74
Extremely Premature, n (%)		4 (26.7%)	8 (53.3%)	0.14
Sex: female (%)/male (%)	6(40.0)/ 9(60.0)	8(53.3)/ 7(46.7)	5(33.3)/ 10(66.7)	0.27
Birth weight, gram, mean (SD)	3275.3 (±440.5)	1129.7 (±328.5)	1101 (±411.9)	0.84
Birth height, centimetre, mean (SD)	50.0 (±1.8)	36.8 (±3.2)	36.5 (±4.7)	0.88
Birth head circumference (cm), mean (SD)	34.4 (±1.3)	26.5 (±3.1)	25.7 (±2.6)	0.45
APGAR score, 1 min (SD)	8.87 (±0.5)	4.93 (±3.4)	5.13 (±2.8)	0.86
APGAR score, 5 min (SD)	9.53 (±0.9)	6.73 (±2.2)	7.87 (±1.2)	0.09
Intrauterine Growth Restriction, n (%)	1 (6.7)	1 (6.7)	4 (66.7)	0.14
Neonatal asphyxia, n (%)	0	0	0	
Bronchopulmonary dysplasia, n (%)	1 (6.7)	5 (33.3)	4 (26.7)	0.69
Intraventricular Haemorrhage (grade 1–2), n (%)	0	4 (26.7%)	1 (6.7%)	0.14
Gestational age at MRI scan, weeks, mean (SD)	39.54 (±1.2)	40.15 (±0.6)	40.48 (±0.6)	0.16
Socio-economic score (range 2–12), mean (SD)	4.10 (±2.5)	6.07 (±3.5)	6.00 (±3.4)	0.96

[a] Group-characteristics were compared using one-way between-subjects ANOVA for continuous variables and chi-squared test for categorical variables.

MRI acquisition was performed on 3.0T Siemens MR scanners (Siemens, Erlangen, Germany): Siemens TIM Trio with a 32-channel head coil and Siemens Prisma with a 64-channel head coil. Chi-squared test revealed no significant difference regarding the distribution of scanner/coils between groups, $\chi(2) = 3.462$, $p = 0.177$ (TIMTrio-32channel: FT = 12, PTM = 8, PTC = 12; Prisma-64channel: FT = 3, PTM = 7, PTC = 3).

T2-weighted images for anatomical reference were acquired using the following parameters: 113 coronal slices, TR = 4990 ms, TE = 151 ms, flip angle = 150°, matrix size = 256x164; voxel size = 0.4x0.4 × 1.2 mm^3, total scan time of 6:01 min.

DTI protocol was acquired with a single-shot spin echo echo-planar imaging (SE-EPI) Stejksal-Tanner sequence (TE = 84 ms, TR = 7400 ms, acquisition matrix 128 × 128 mm, reconstruction matrix 128 × 128mm, 60 slices, voxel size 2x2x2mm^3). Images were acquired in the axial plane, in anterior-posterior (AP) phase encoding (PE) direction, with diffusion gradients applied in 30 non-collinear directions with a b-value of 1000 s/mm^2 and one non-diffusion weighted image (b = 0), with a total scan time of 4:12 min.

2.4. Pre-processing

DTI data were preprocessed using the diffusion toolbox of the FMRIB Software Library, FSL v5.0.10, https://fsl.fmrib.ox.ac.uk/fsl/fslwiki/(Behrens et al., 2003; Smith et al., 2004). Eddy current-induced distortions and gross subject movement were corrected using the FSL "eddy" tool (Andersson and Sotiropoulos, 2016), which included a function optimized for neonatal diffusion data regarding correction of distortions caused by motion-induced signal dropout and intra-volume

subject movement (Andersson et al., 2016, 2017; Bastiani et al., 2019).

2.5. Data analysis

2.5.1. ROI analysis

20 ROI situated in the WM were manually drawn on a study-specific template. This template was generated using DTI-TK (http://www.nitrc.org/projects/dtitk), a toolkit used for tensor-based spatial normalization of diffusion MRI data to an iteratively optimized study-specific template (Zhang et al., 2006). First, we created a study-specific template by choosing one subject and registering all the subjects to that particular one. Then, we re-registered all subjects to this newly generated template in order to obtain our final study-specific template where we drew the 20 ROI. The study-specific template and details regarding its construction can be found in Supplementary Material Fig. S2. The 20 ROI drawn on this template were back transformed to each subject's space in order to compute ROI-average estimates of DTI measures (FA, MD, AD, RD) per subject using FSL DTIFIT. Besides the ROI-average DTI estimates per subject, global DTI average measures (FA, MD, AD, RD) were obtained for each subject by averaging the mean DTI measures of all 20 ROI. The 20 ROI were the following: splenium of corpus callosum (cc-sp), body of corpus callosum (cc-bd), genu of corpus callosum (cc-ge), superior corona radiata (scr), forceps minor (fmin), anterior commissure (ac), forceps major (fmaj), posterior limb of the internal capsule (plic), anterior limb of the internal capsule (alic), inferior longitudinal fasciculus (ilf), external capsule/claustrum/extreme capsule (ec), superior longitudinal fasciculus (slf), optic radiation (or), acoustic radiation (ar), frontal gyrus white matter (fg-wm), arcuate fasciculus (af), superior temporal gyrus white matter (stg-wm), medial temporal gyrus white matter (mtg-wm), cingulum (cg) and fornix (fx), (Supplementary Fig. S3).

2.5.2. Tractography analysis

In the context of this study, a hypothesis-based tractography approach was chosen and three tracts were reconstructed using seed-based probabilistic tractography performed with FSL v5.0.10 (Behrens et al., 2003; Smith et al., 2004): acoustic radiations, interhemispheric temporal callosal fibers (both involved in the processing of auditory information) and the uncinate fasciculus (known to be implicated in socio-emotional processing) (Supplementary Fig. S4). Fiber orientation distributions (FOD) were estimated using the model-based approach available in FSL's Bedpostx (Behrens et al., 2007). This method runs Markov Chain Monte Carlo sampling to build up distributions on FOD parameters at each voxel, with up to three fiber compartments estimated in each voxel, allowing the automatic detection of the number of crossing fibres per voxel. Following Bedpostx, seed-based probabilistic tractography was performed using Probtrackx2 (Behrens et al., 2007), computing 5000 streamlines from each seed voxel.

Given the specificity of our population and of the tracts we aimed to reconstruct, we performed tractography in the subject's native diffusion space using manually-placed masks. Therefore, sets of "seed" (regions where the tract starts), "waypoint" (regions through which tracts should go through), "stop" (regions where tracts terminate) and "exclusion" (regions that tracts should avoid) masks were drawn manually directly in the subject diffusion space, always by the same operator, blinded for the groups, and in the same manner for all subjects (the same masks were selected per tract for each subject). Tractography results obtained for each subject were thresholded at 0.01 and binarized to obtain tract-specific masks. DTI metrics (FA, MD, AD and RD) were calculated in each subject's diffusion space for each tract using the obtained masks.

Masks for each tract were drawn according to published literature and atlases (Adibpour et al., 2018; Akazawa et al., 2016; Oishi et al., 2010) and were designed as follows. For the left and right acoustic radiations, a seed mask was placed in primary auditory cortex (either left or right) in the temporal lobe and a waypoint mask was placed in the ipsilateral thalamus medial geniculate nucleus; an exclusion mask was generated to restrict the pathway to the hemisphere ipsilateral to the seed mask and exclude ipsilateral optic radiations fibers. For the interhemispheric temporal callosal fibers, two seeds were used, comprising the left and right primary auditory cortex and a waypoint in the splenium of corpus callosum; an exclusion mask was generated to exclude ipsilateral optic radiations and fibers of the posterior limb of internal capsule. For the left and right uncinate fasciculus, a first seed was placed in the temporal lobe (either right or left) and a second seed was placed in the ipsilateral inferior part of the frontal lobe; the seed masks were also used as waypoint masks; an exclusion mask was generated to restrict the pathway to the hemisphere ipsilateral to the seed mask and exclude fibers from the posterior limb of internal capsule (Supplementary Fig. S5).

2.5.3. Amygdala Volumetric analysis

To evaluate differences regarding amygdala volumes between PTM, PTC and FT newborns, amygdala was segmented on T2-weighted images. Segmentation was manually performed by a single rater using the manual contour editing function of ITK-SNAP visualization software (Yushkevich et al., 2006), based on anatomical guidelines for the localization of amygdala, according to published literature and to a neonatal atlas describing a protocol for amygdala manual segmentation (Cismaru et al., 2016; Gousias et al., 2012). All segmentations were validated by a neurosurgeon with expertise in neuroanatomy. With the 0.4x0.4 $\times$ 1.2 mm^3 voxel size resolution, amygdala delineation ran through approximately 8 coronal slices, 28 sagittal slices and 28 axial slices, which was deemed to enable a good visualization of the structure by the expert neurosurgeon. Additionally, intracranial cavity (ICC) volumes were obtained from the T2-weighted images of each subject with an automatic neonatal brain segmentation method (Gui et al., 2012). Out of the 45 patients, only 34 could be used for the analysis, due to movement in T2-weighted images, preventing correct delineation of amygdala limits (Supplementary Fig. S6).

2.6. Statistical analysis

All statistical analyses were performed with IBM SPSS Statistics version 25 (IBM Corp., Armonk, N.Y., USA).

Regarding neonatal and demographic data, categorical variables (sex, cases of extremely premature, intrauterine growth restriction, bronchopulmonary dysplasia and intraventricular haemorrhage grade 1 and 2) were analysed using chi-squared test, whereas continuous variables were compared using one-way between-subjects ANOVA, with group (FT, PTC, PTM) as independent variable and the following dependent variables: GA at birth, GA at MRI, birth weight, birth height, birth head circumference, APGAR score at 1 and 5 min after birth and socio-economic parental status.

The global mean DTI metrics, obtained by averaging the 20 ROI per subject, were analysed by means of one-way between-subjects ANCOVA to investigate differences in global DTI metrics (FA, MD, RD and AD) between FT, PTM and PTC groups, controlling for GA at MRI. Additionally, DTI metrics per ROI were analysed by means of one-way between-subjects MANCOVA to study significant differences between FT, PTM and PTC groups on the mean FA, MD, RD and AD of each ROI, controlling for GA at MRI. Sex was not a significant predictor for any of the dependent variables, which is why it was not included as a co-variable in the final analysis.

Regarding tractography results of interhemispheric temporal callosal fibers, one-way between-subjects ANCOVA, controlling for GA at MRI, was conducted to determine the statistically significant differences between FT, PTM and PTC groups on mean FA, MD, RD and AD. For acoustic radiations and uncinate fasciculus tractography results, a two-way between-subjects ANCOVA, controlling for GA at MRI, was conducted to investigate statistically significant differences in mean DTI metrics (FA, MD, RD and AD) between FT, PTM and PTC groups, as well as between left and right hemisphere. Sex was not a significant predictor for any of the dependent variables, which is why it was not included as a

co-variable in the final analysis. Additionally, hemispheric asymmetries within each group were investigated by conducting paired-samples t-tests comparing mean DTI metrics of the left- and right-hemisphere fiber tracts per group.

Group differences in amygdala volumes were analysed using two-way between-subjects ANCOVA, with amygdala volume as dependent variable, ICC volume, GA at MRI and sex as covariates, and group (FT, PTM and PTC) and hemisphere (right and left) as independent variables. Hemispheric asymmetries were investigated with paired-samples t-tests, comparing left- and right-hemisphere amygdala volumes within each group.

One-way and two-way between-subjects ANOVA, ANCOVA and MANCOVA results were corrected for multiple comparisons, using Bonferroni post hoc test correction.

2.7. Data and code availability

All data were acquired in the context of the research project approved by the ethical committee in 2011.

Patient consent form did not include any clause for reuse or share of data. It stated explicitly that all data (clinic, biologic and imaging) would not be used with any other aim apart from the present research study and would not be shared with third parties.

Software and code used in this study are publicly available as part of: FSL v5.0.10 (https://fsl.fmrib.ox.ac.uk/fsl/fslwiki/) and DTI-TK (http://www.nitrc.org/projects/dtitk) toolkits. Diffusion MRI data was processed using the developing Human Connectome Project (dHCP, http://www.developingconnectome.org) neonatal diffusion MRI automated pipeline, which can be found at this link: https://git.fmrib.ox.ac.uk/matteob/dHCP_neo_dMRI_pipeline_release (Bastiani et al., 2019).

3. Results

3.1. ROI analysis

First, whole-brain WM maturation per group was investigated using global DTI metrics (FA, MD, RD and AD averaged between all 20 ROI per subject). Our analysis revealed a statistically significant difference

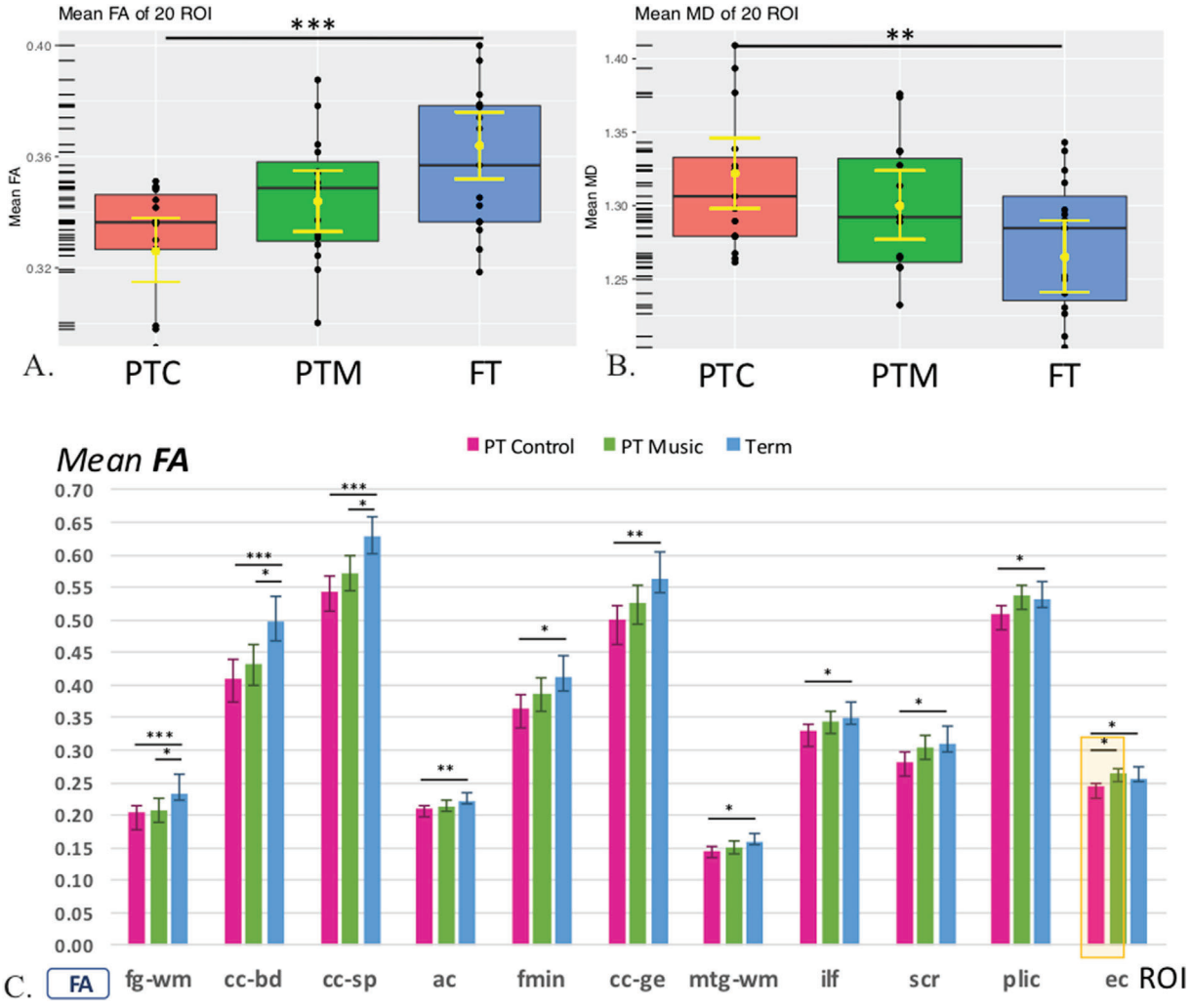

Fig. 1. Illustration of results from the statistical analysis of ROI-based DTI metrics. A - Boxplot of global mean FA over all ROI with mean and 95% confidence intervals (in yellow); B - Boxplot of global mean MD over all ROI with mean and 95% confidence intervals (in yellow); One-way between-subjects ANCOVA with correction for gestational age at MRI was performed with Bonferroni post hoc test. C - Bar graph of mean FA per ROI (mean and 95% confidence intervals) in 11 of the 20 ROI where statistical differences between groups were found. One-way between-subjects MANCOVA with correction for gestational age at MRI was performed with Bonferroni post hoc test. Lines indicate significant differences between groups (*$p < 0.05$, **$p < 0.01$, ***$p < 0.001$). ROI abbreviations: fg-wm - frontal gyrus white matter, cc-bd - body of corpus callosum, cc-sp - splenium of corpus callosum, ac - anterior commissure, fmin - forceps minor, cc-ge - genu of corpus callosum, mtg-wm - medial temporal gyrus white matter, ilf - inferior longitudinal fasciculus, scr - superior corona radiata, plic - posterior limb of the internal capsule, ec - external capsule/claustrum/extreme capsule.

between FT, PTM and PTC on the global mean FA, [F(2,41) = 9.285, p = 0.0001], global mean MD, [F(2,41) = 5.157, p = 0.01] and global mean RD [F(2,41) = 6.706, p = 0.003]. After Bonferroni post hoc correction, PTC had a significantly lower global FA (p = 0.0001) and a significantly higher global MD (p = 0.008) and RD (p = 0.002) than FT newborns, while PTM showed no significant difference in any of DTI metrics in comparison to FT infants (Fig. 1A, Fig. 1B, Tables 2 and 3).

Second, we analysed group differences in WM maturation in each ROI. Considering all the regions at the same time, one-way MANCOVA multivariate test yielded a significant difference between the group contrasts, [Wilks'λ = 0.147, F(40,44) = 1.770, p = 0.033]. Given the significance of the overall test, the univariate main effects were examined. There was a statistically significant difference between FT, PTM and PTC on mean FA in 11 of the 20 ROI: "cc-sp", "cc-bd", "cc-ge", "scr", "fmin", "ac", "plic", "ilf", "ec", "mtg-wm" and "fg-wm". Bonferroni post hoc test showed that mean FA was significantly reduced in PTC vs FT newborns in 11 ROI: "cc-sp" (p = 0.0001), "cc-bd" (p = 0.001), "cc-ge" (p = 0.003), "scr" (p = 0.043), "fmin" (p = 0.011), "ac" (p = 0.01), "plic" (p = 0.045), "ilf" (p = 0.024), "ec" (p = 0.019), "fg-wm" (p = 0.006) and "mtg-wm" (p = 0.02). In contrast, mean FA was significantly reduced in PTM vs FT newborns in only 3 ROI: "cc-sp" (p = 0.016), "cc-bd" (p = 0.011) and "fg-wm" (p = 0.027), and no significant difference was detected between PTM and FT infants in the other ROI. Moreover, in the "ec" ROI, FA was significantly higher in PTM vs PTC (p = 0.01) (Fig. 1C, Table 2).

In order to further explore the reduction of FA in preterm newborns vs full-term infants, we analysed the MD, RD and AD of those 11 ROI. In comparison to FT infants, PTC had a significantly higher MD in "cc-sp", "cc-bd", "ilf" and "fg-wm"; as well as a significantly higher RD in "cc-sp", "cc-bd", "cc-ge", "fmin", "ac", "ilf" and "fg-wm", and a significantly lower AD in "plic". PTM, in comparison to FT newborns, presented a significantly higher MD only in "cc-sp", a significantly higher RD in "cc-sp" and "cc-bd" and a significantly higher AD in "fg-wm". In the ROI "scr", "ec" and "mtg-wm" there were no significant differences regarding MD, RD or AD between groups (Table 3).

Effect size between groups in each region were calculated by means of Cohen's d, revealing a high practical significance (d > 0.8) between groups in all the regions where p≤0.05 (Supplementary Tables S1 and S2).

3.2. Tractography analysis

The analysis of the left and right acoustic radiations tractography data resulted in a statistically significant difference between FT, PTM and PTC on mean FA, [F(2,82) = 4.216, p = 0.018]. Bonferroni post hoc test showed that mean FA was significantly higher in PTM vs PTC newborns (p = 0.023). There was no statistically significant difference between the three groups in mean MD, [F(2,82) = 0.619, p = 0.481], mean RD [F(2,82) = 0.942, p = 0.394] and mean AD [F(2,82) = 1.341, p = 0.267] (Fig. 2A, Fig. 2B, Table 4). Moreover, there was no significant difference regarding mean FA, MD, RD and AD between left and right acoustic radiations, neither when considering the three groups together, nor when evaluating per group (Table 4 and Supplementary Table S3).

Regarding interhemispheric temporal callosal fibers, our analysis revealed a statistically significant difference between FT, PTM and PTC in mean FA [F(2,40) = 5.879, p = 0.006], as well as in mean MD [F(2,41) = 9.248, p = 0.001], mean RD [F(2,41) = 5.681, p = 0.007] and mean AD [F(2,41) = 12.450, p = 0.0001]. Bonferroni post hoc test showed that, in comparison to FT newborns, PTC evidenced a significantly lower FA (p = 0.004), higher MD (p = 0.001), higher RD (p = 0.008) and higher AD (p = 0.04); while PTM presented no significant difference in FA or AD compared to FT infants, but a significantly higher mean MD (p = 0.018) and RD (p = 0.033). Additionally, in comparison to PTC, PTM exhibited a lower AD (p = 0.0001) (Fig. 2C and D, Table 4).

Tractography analysis of the left and right uncinate fasciculus revealed a statistically significant difference between FT, PTM and PTC on mean FA [F(2,82) = 6.802, p = 0.001], mean MD [F(2,82) = 8.311, p = 0.001], mean RD [F(2,82) = 5.133, p = 0.008] and mean AD [F(2,82) = 10.391, p = 0.0001]. Bonferroni post hoc test showed that, in comparison to FT newborns, PTC had a significantly lower FA (p = 0.004),

Table 2
Corrected global mean FA (of the averaged 20 ROI) with differences between groups calculated using one-way between-subjects ANCOVA and corrected mean FA of each ROI with differences between groups calculated using one-way between-subjects MANCOVA. Numbers in bold indicate significant results between groups (p < 0.05) and pairwise comparisons that survived Bonferroni post hoc test (p≤0.05).

ROI	Mean FA (95% CI)			Statistical Results			
	Full-term	Preterm Music	Preterm Control	Group effect (p)	Pairwise comparison (p)		
					FT vs PTC	FT vs PTM	PTM vs PTC
Average all 20 ROI	0.364 (0.352–0.376)	0.344 (0.333–0.355)	0.326 (0.315–0.338)	**0.0001**	**0.0001**	0.058	0.106
cc-sp	0.630 (0.602–0.659)	0.573 (0.546–0.600)	0.540 (0.513–0.568)	**0.0001**	**0.0001**	**0.016**	0.282
cc-bd	0.503 (0.469–0.536)	0.432 (0.400–0.463)	0.406 (0.373–0.439)	**0.001**	**0.001**	**0.011**	0.781
cc-ge	0.573 (0.542–0.605)	0.523 (0.494–0.553)	0.492 (0.461–0.523)	**0.004**	**0.003**	0.76	0.434
scr	0.316 (0.296–0.336)	0.303 (0.285–0.322)	0.279 (0.260–0.298)	**0.041**	**0.043**	1	0.223
fmin	0.419 (0.392–0.445)	0.385 (0.360–0.410)	0.359 (0.333–0.385)	**0.014**	**0.011**	0.224	0.454
ac	0.226 (0.217–0.235)	0.214 (0.205–0.222)	0.206 (0.197–0.215)	**0.013**	**0.01**	0.153	0.597
fmaj	0.508 (0.479–0.538)	0.489 (0.461–0.517)	0.468 (0.439–0.497)	0.186	0.206	1	0.914
plic	0.539 (0.519–0.558)	0.535 (0.517–0.554)	0.503 (0.484–0.522)	**0.022**	**0.045**	1	0.051
alic	0.344 (0.324–0.363)	0.337 (0.319–0.355)	0.325 (0.306–0.344)	0.404	0.569	1	1
ilf	0.358 (0.340–0.375)	0.342 (0.325–0.359)	0.322 (0.305–0.340)	**0.028**	**0.024**	0.588	0.303
ec	0.262 (0.251–0.274)	0.262 (0.252–0.273)	0.238 (0.227–0.250)	**0.005**	**0.019**	1	**0.01**
slf	0.301 (0.285–0.318)	0.299 (0.283–0.314)	0.287 (0.271–0.303)	0.420	0.694	1	0.842
or	0.321 (0.299–0.344)	0.300 (0.279–0.320)	0.288 (0.266–0.309)	0.117	0.125	0.472	1
ar	0.265 (0.252–0.277)	0.277 (0.265–0.289)	0.265 (0.253–0.277)	0.252	1	0.484	0.483
fg-wm	0.243 (0.223–0.262)	0.206 (0.188–0.225)	0.197 (0.178–0.216)	**0.005**	**0.006**	**0.027**	1
af	0.271 (0.251–0.292)	0.251 (0.232–0.271)	0.240 (0.220–0.261)	0.123	0.132	0.493	1
stg-wm	0.214 (0.204–0.223)	0.206 (0.197–0.215)	0.199 (0.190–0.208)	0.113	0.113	0.697	0.851
mtg-wm	0.163 (0.154–0.172)	0.151 (0.142–0.160)	0.144 (0.135–0.153)	**0.023**	**0.02**	0.188	0.795
cg	0.344 (0.330–0.359)	0.331 (0.317–0.345)	0.329 (0.314–0.343)	0.284	0.434	0.561	1
fx	0.475 (0.434–0.516)	0.460 (0.421–0.499)	0.441 (0.401–0.482)	0.529	0.794	1	1

cc-sp - splenium of corpus callosum, cc-bd - body of corpus callosum, cc-ge - genu of corpus callosum, scr - superior corona radiata, fmin - forceps minor, ac – anterior commissure, fmaj - forceps major, plic - posterior limb of the internal capsule, alic - anterior limb of the internal capsule, ilf - inferior longitudinal fasciculus, ec - external capsule/claustrum/extreme capsule, slf - superior longitudinal fasciculus, or - optic radiation, ar - acoustic radiation, fg-wm - frontal gyrus white matter, af - arcuate fasciculus, stg-wm - superior temporal gyrus white matter, mtg-wm - medial temporal gyrus white matter, cg - cingulum, fx - fornix; CI - confidence interval; (p) - p-value.

Table 3
Corrected global mean MD, RD and AD (of the averaged 20 ROI) with differences between groups calculated using one-way between-subjects ANCOVA, and corrected mean MD, RD and AD of the 11 ROI where FA was statistically different between groups, with differences between groups calculated using one-way between-subjects MANCOVA. Numbers in bold indicate significant results between groups ($p<0.05$) and pairwise comparisons that survived Bonferroni post hoc test ($p\leq 0.05$).

		Mean DTI measurements (95% CI)			Statistical Results			
ROI		*Full-term*	*Preterm Music*	*Preterm Control*	*Group effect (p)*	*Pairwise comparison (p)*		
						FT vs PTC	*FT vs PTM*	*PTM vs PTC*
Mean MD of all 20 ROI		1.265 (1.241-1.290)	1.300 (1.277-1.324)	1.322 (1.298-1.346)	**0.01**	**0.008**	0.134	0.566
Mean RD of all 20 ROI		1.000 (0.970-1.029)	1.045 (1.018-1.073)	1.078 (1.049-1.107)	**0.003**	**0.002**	0.089	0.319
Mean AD of all 20 ROI		1.796 (1.777-1.816)	1.810 (1.792-1.829)	1.811 (1.792-1.831)	0.513			
cc-sp	*MD*	1.199 (1.154-1.245)	1.283 (1.288-1.375)	1.346 (1.301-1.390)	**0.0001**	**0.0001**	**0.033**	0.140
	RD	0.693 (0.638-0.748)	0.807 (0.755-0.859)	0.886 (0.832-0.940)	**0.0001**	**0.0001**	**0.014**	0.109
	AD	2.212 (2.157-2.266)	2.236 (2.185-2.287)	2.264 (2.211-2.318)	0.414			
cc-bd	*MD*	1.255 (1.209-1.301)	1.331 (1.288-1.375)	1.382 (1.337-1.427)	**0.002**	**0.001**	0.06	0.317
	RD	0.863 (0.804-0.921)	0.987 (0.932-1.042)	1.050 (0.993-1.107)	**0.0001**	**0.0001**	**0.010**	0.339
	AD	2.039 (1.967-2.111)	2.020 (1.952-2.088)	2.047 (1.976-2.117)	0.850			
cc-ge	*MD*	1.244 (1.190-1.298)	1.287 (1.236-1.337)	1.336 (1.284-1.389)	0.072			
	RD	0.782 (0.715-0.849)	0.862 (0.798-0.925)	0.929 (0.864-0.995)	**0.016**	**0.013**	0.279	0.419
	AD	2.168 (2.123-2.213)	2.136 (2.094-2.179)	2.150 (2.106-2.195)	0.605			
scr	*MD*	1.200 (1.154-1.246)	1.219 (1.175-1.262)	1.268 (1.223-1.313)	0.110			
	RD	0.982 (0.932-1.031)	1.007 (0.960-1.053)	1.065 (1.017-1.114)	0.064			
	AD	1.636 (1.589-1.683)	1.642 (1.598-1.687)	1.674 (1.628-1.720)	0.472			
fmin	*MD*	1.366 (1.321-1.411)	1.407 (1.365-1.450)	1.444 (1.399-1.488)	0.073			
	RD	1.020 (0.962-1.079)	1.084 (1.029-1.140)	1.136 (1.078-1.193)	**0.034**	**0.029**	0.360	0.588
	AD	2.059 (2.025-2.092)	2.053 (2.022-2.084)	2.059 (2.026-2.091)	0.956			
ac	*MD*	1.100 (1.070-1.129)	1.141 (1.114-1.169)	1.156 (1.127-1.185)	0.033			
	RD	0.967 (0.939-0.995)	1.010 (0.984-1.036)	1.027 (0.999-1.055)	**0.016**	**0.016**	0.097	1
	AD	1.365 (1.328-1.401)	1.404 (1.370-1.438)	1.413 (1.378-1.449)	0.159			
plic	*MD*	1.021 (1.005-1.037)	1.006 (0.990-1.021)	1.018 (1.002-1.034)	0.313			
	RD	0.670 (0.646-0.694)	0.664 (0.642-0.686)	0.698 (0.675-0.721)	0.097			
	AD	1.723 (1.695-1.751)	1.688 (1.662-1.715)	1.659 (1.631-1.686)	**0.011**	**0.009**	0.234	0.364
ilf	*MD*	1.361 (1.320-1.402)	1.387 (1.348-1.426)	1.439 (1.399-1.479)	**0.037**	**0.039**	1	0.197
	RD	1.077 (1.032-1.122)	1.113 (1.071-1.155)	1.174 (1.130-1.218)	**0.015**	**0.014**	0.748	0.137
	AD	1.930 (1.883-1.977)	1.936 (1.891-1.980)	1.969 (1.923-2.015)	0.455			
ec	*MD*	1.188 (1.165-1.211)	1.203 (1.182-1.225)	1.200 (1.177-1.223)	0.614			
	RD	1.033 (1.008-1.058)	1.048 (1.024-1.071)	1.062 (1.037-1.086)	0.296			
	AD	1.498 (1.471-1.524)	1.515 (1.490-1.540)	1.477 (1.451-1.503)	0.112			
fg-wm	*MD*	1.356 (1.302-1.410)	1.464 (1.414-1.515)	1.458 (1.405-1.511)	**0.011**	**0.037**	**0.017**	1
	RD	1.208 (1.147-1.270)	1.329 (1.271-1.387)	1.331 (1.271-1.391)	**0.011**	**0.026**	**0.020**	1
	AD	1.651 (1.609-1.693)	1.735 (1.696-1.774)	1.712 (1.671-1.753)	**0.018**	0.146	**0.016**	1
mtg-wm	*MD*	1.402 (1.366-1.439)	1.435 (1.400-1.469)	1.427 (1.391-1.463)	0.431			
	RD	1.296 (1.257-1.334)	1.334 (1.298-1.370)	1.329 (1.292-1.367)	0.321			
	AD	1.616 (1.580-1.652)	1.638 (1.604-1.671)	1.622 (1.587-1.657)	0.657			

cc-sp - splenium of corpus callosum, cc-bd - body of corpus callosum, cc-ge - genu of corpus callosum, scr - superior corona radiata, fmin - forceps minor, ac - anterior commissure, plic - posterior limb of the internal capsule, ilf– inferior longitudinal fasciculus, ec - external capsule/claustrum/extreme capsule, fg-wm - frontal gyrus white matter, mtg-wm - medial temporal gyrus white matter; CI - confidence interval; (p) - p-value.

while PTM presented a significantly lower MD ($p = 0.001$), RD ($p = 0.018$) and AD ($p = 0.0001$). Additionally, in comparison to PTC, PTM had a significantly higher FA ($p = 0.03$) and a significantly lower MD ($p = 0.01$), RD ($p = 0.037$) and AD ($p = 0.05$) (Fig. 2E and F, Table 4). There was no significant difference in mean FA, MD, RD and AD between the left and right uncinate fasciculi, neither when considering the three groups together, nor when evaluating per group (Table 4 and Supplementary Table S3).

Effect size between groups in each region were calculated by means of Cohen's, revealing a moderate to high practical significance ($0.592 \leq d \leq 1.482$) in all the regions where $p \leq 0.05$ (Supplementary Table S4).

3.3. Amygdala volumetric analysis

Amygdala volumetric statistical analysis showed a statistically significant difference between FT, PTM and PTC, [$F(2,59) = 8.833$, $p = 0.0001$], correcting for GA at MRI, sex and ICC volumes. Bonferroni post hoc test showed that amygdala volumes were significantly smaller in PTC vs FT ($p = 0.001$), whereas PTM had significantly larger amygdala volumes vs PTC ($p = 0.006$), and not significantly different from FT newborns (Fig. 3, Table 5). There were no significant differences between left and right amygdala volumes, neither when considering the three groups together, nor when evaluating per group (Table 5 and Supplementary Table S5).

Effect size between groups regarding amygdala volumes were calculated by means of Cohen's d, revealing a moderate to high practical significance ($0.718 \leq d \leq 1.285$) where $p \leq 0.05$ (Supplementary Table S6).

4. Discussion

The aim of the present study was to evaluate the effect of an early postnatal music intervention during NICU stay on VPT infants' brain structural maturation. Music has been proven to elicit changes in limbic

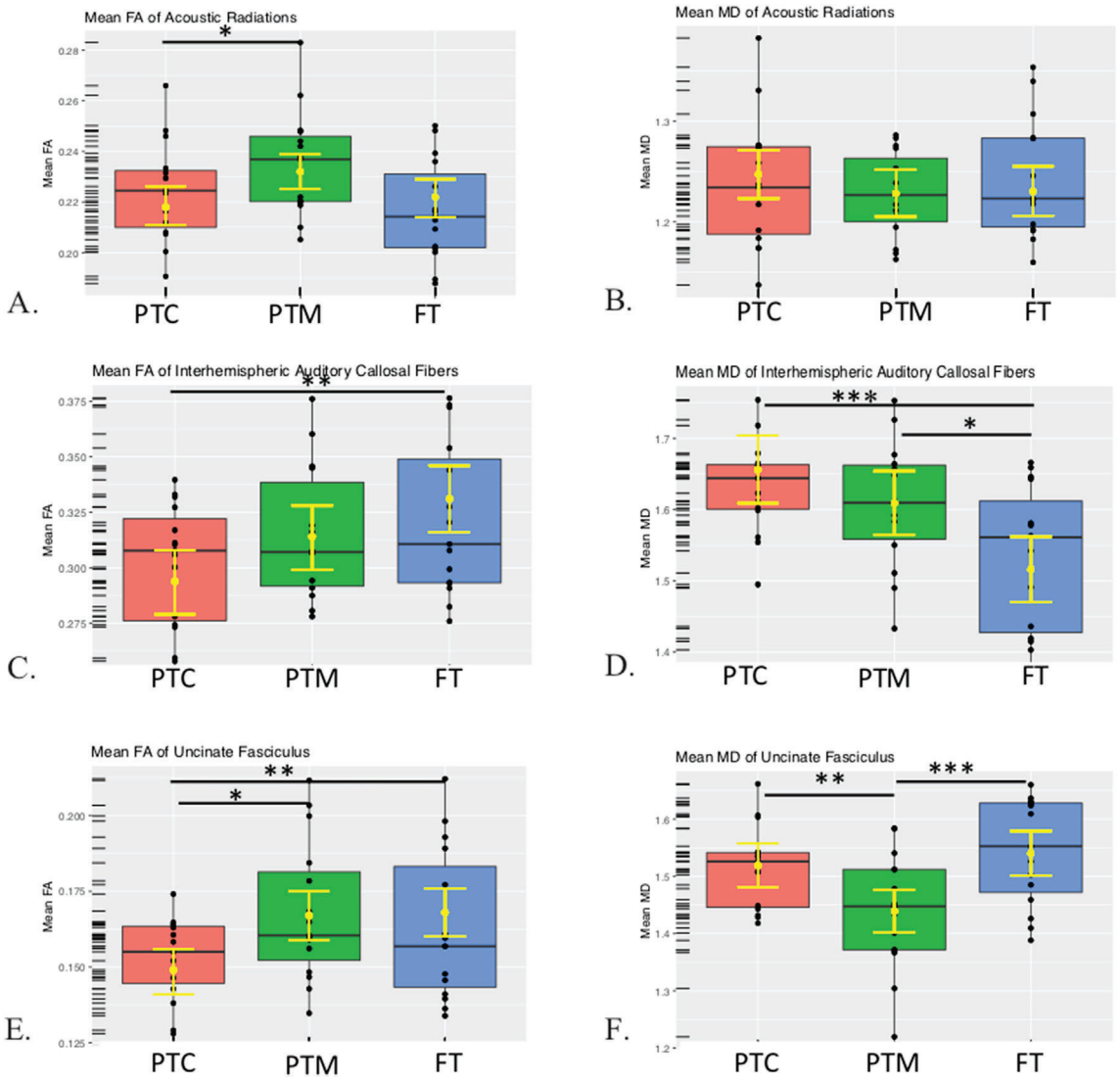

Fig. 2. Analysis of DTI metrics of tracts obtained via tractography. A - Boxplot of mean FA for acoustic radiations; Two-way between-subjects ANCOVA with correction for gestational age at MRI was performed. Left and right fasciculi differences are not shown. B- Boxplot of mean MD for acoustic radiations; Two-way between-subjects ANCOVA with correction for gestational age at MRI was performed. Left and right fasciculi differences are not shown. C - Boxplot of mean FA for interhemispheric temporal callosal fibers; One-way between-subjects ANCOVA with correction for gestational age at MRI was performed. D - Boxplot of mean MD for interhemispheric temporal callosal fibers; One-way between-subjects ANCOVA with correction for gestational age at MRI was performed. E – Boxplot of mean FA for uncinate fasciculus; Two-way between-subjects ANCOVA with correction for gestational age at MRI was performed. Left and right fasciculi differences are not shown. F- Boxplot of mean MD for uncinate fasciculus; Two-way between-subjects ANCOVA with correction for gestational age at MRI was performed. Left and right fasciculi differences are not shown. All analyses were performed with Bonferroni post hoc test. Mean and 95% confidence intervals are illustrated in yellow on each boxplot. Lines indicate significant differences between groups (*$p < 0.05$, **$p < 0.01$, ***$p < 0.001$).

and paralimbic brain functional networks that are involved in socio-emotional processing in both adults (Blood and Zatorre, 2001; Koelsch, 2014) and in newborn infants (Lordier, 2019; Perani et al., 2010).

We therefore hypothesized that an early music intervention in VPT infants could have an effect on VPT infants' macro and microstructural brain development, in particular regarding cortico-limbic networks.

To study these structural brain effects of an early music intervention, we assessed brain WM maturation, using DTI, in 20 different regions defined across the whole-brain WM and specifically in tracts involved in auditory and socio-emotional processing (acoustic radiations, inter-hemispheric temporal callosal fibers and uncinate fasciculus). Furthermore, we investigated the effect of the music intervention on the amygdala volume – an integral part of the limbic system which plays a central role in emotion modulation during music processing (Ball et al., 2007; Blood and Zatorre, 2001; Koelsch et al., 2013; Koelsch, 2014).

4.1. Regional effects of prematurity and music intervention on WM maturation

Our ROI-based analysis revealed that VPT infants who received standard-of-care and without signs of brain lesions on conventional MRI, when at TEA, show an overall decreased WM maturation in comparison to FT newborns, with several regions of diminished FA and/or higher diffusivity when compared to FT newborns.

The brain areas that we found to be affected by prematurity are similar to the ones described in the existing literature, comprising "fg-wm", "cc-sp", "cc-bd", "cc-ge", "plic", "ilf", "ec" and "scr" (Akazawa et al., 2016; Anjari et al., 2007; Dyet et al., 2006; Huppi et al., 1998; Rose et al., 2008; Thompson et al., 2011). Besides these regions, we show, to the best of our knowledge, for the first time, that PTC at TEA also present a diminished FA and/or higher diffusivity in "ac", "fmin" and "mtg-wm", in

Table 4
Corrected mean FA, MD, RD and AD for acoustic radiations, interhemispheric temporal callosal fibers and uncinate fasciculus, with groups differences calculated using one-way and two-way between-subjects ANCOVA. Numbers in bold indicate significant results between groups ($p<0.05$) and pairwise comparisons that survived Bonferroni post hoc test ($p\leq0.05$).

ROI	*Full-term*	*Preterm Music*	*Preterm Control*	*Statistical Results*			
				Group effect (p)	*Pairwise comparison (p)*		
					FT vs PTC	*FT vs PTM*	*PTM vs PTC*
	Mean FA (95% CI)						
Ac. Rad. average	0.222 (0.214-0.229)	0.232 (0.225-0.239)	0.218 (0.211-0.226)	**0.018**	1	0.133	**0.023**
Left	0.221 (0.211-0.231)	0.231 (0.221-0.241)	0.219 (0.209-0.230)	0.845			
Right	0.222 (0.212-0.233)	0.234 (0.224-0.244)	0.217 (0.207-0.228)				
Interhemispheric Temp. Call. Fib.	0.331 (0.316-0.346)	0.314 (0.299-0.328)	0.294 (0.279-0.308)	**0.006**	**0.004**	0.323	0.170
Unc. F. average	0.168 (0.160-0.176)	0.167 (0.159-0.175)	0.149 (0.141-0.156)	**0.001**	**0.004**	1	**0.03**
Left	0.168 (0.157-0.179)	0.166 (0.155-0.177)	0.149 (0.138-0.160)	0.908			
Right	0.168 (0.157-0.179)	0.168 (0.157-0.179)	0.148 (0.137-0.159)				
	Mean MD (95% CI)						
Ac. Rad. average	1.230 (1.206-1.255)	1.228 (1.205-1.252)	1.247 (1.223-1.271)	0.481			
Left	1.217 (1.183-1.250)	1.241 (1.208-1.273)	1.249 (1.216-1.282)	0.978			
Right	1.244 (1.210-1.277)	1.216 (1.183-1.249)	1.246 (1.212-1.279)				
Interhemispheric Temp. Call. Fib.	1.516 (1.470-1.562)	1.609 (1.564-1.654)	1.656 (1.609-1.704)	**0.001**	**0.001**	**0.018**	0.441
Unc. F. average	1.540 (1.501-1.579)	1.439 (1.402-1.476)	1.519 (1.481-1.557)	**0.001**	1	**0.001**	**0.01**
Left	1.554 (1.501-1.608)	1.449 (1.397-1.501)	1.534 (1.481-1.587)	0.229			
Right	1.526 (1.472-1.579)	1.429 (1.377-1.482)	1.504 (1.451-1.557)				
	Mean RD (95% CI)						
Ac. Rad. average	1.091 (1.066-1.116)	1.083 (1.059-1.106)	1.106 (1.081-1.131)	0.394			
Left	1.078 (1.044-1.113)	1.090 (1.057-1.124)	1.104 (1.070-1.139)	0.712			
Right	1.105 (1.070-1.139)	1.075 (1.042-1.109)	1.108 (1.073-1.143)				
Interhemispheric Temp. Call. Fib.	1.245 (1.188-1.302)	1.349 (1.296-1.403)	1.377 (1.321-1.433)	**0.007**	**0.008**	**0.033**	1
Unc. F. average	1.418 (1.375-1.461)	1.333 (1.293-1.374)	1.408 (1.366-1.451)	**0.008**	1	**0.018**	**0.037**
Left	1.424 (1.365-1.482)	1.341 (1.284-1.398)	1.414 (1.356-1.473)	0.584			
Right	1.412 (1.353-1.471)	1.326 (1.269-1.383)	1.402 (1.342-1.462)				
	Mean AD (95% CI)						
Ac. Rad. average	1.511 (1.483-1.538)	1.540 (1.515-1.566)	1.536 (1.509-1.563)	0.267			
Left	1.496 (1.459-1.534)	1.549 (1.513-1.585)	1.538 (1.502-1.575)	0.908			
Right	1.525 (1.459-1.534)	1.531 (1.495-1.568)	1.533 (1.495-1.571)				
Interhemispheric Temp. Call. Fib.	2.057 (2.001-2.113)	1.976 (1.923-2.029)	2.162 (2.107-2.216)	**0.0001**	**0.04**	0.124	**0.0001**
Unc. F. average	1.811 (1.773-1.850)	1.690 (1.654-1.726)	1.754 (1.716-1.792)	**0.0001**	0.143	**0.0001**	**0.050**
Left	1.824 (1.771-1.876)	1.696 (1.645-1.748)	1.767 (1.715-1.819)	0.315			
Right	1.799 (1.746-1.852)	1.683 (1.632-1.735)	1.741 (1.687-1.795)				

Ac. Rad. – acoustic radiations, Interhemispheric Temp. Call. Fib. – Interhemispheric temporal callosal fibers, Unc. F. – uncinate fasciculus; CI - confidence interval; (p) - p-value.

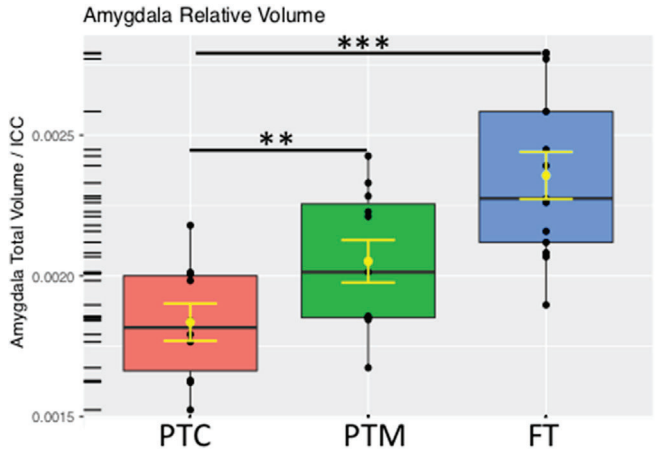

Fig. 3. Boxplot representing the distribution of total amygdala volume (left and right) relative to the ICC volume per group. Mean and 95% confidence intervals are illustrated in yellow. Lines indicate significant differences between groups that survived two-way between-subjects ANCOVA analysis with Bonferroni post hoc test correction; (*$p < 0.05$, **$p < 0.01$, ***$p < 0.001$). The analysis was performed using as covariates: gestational age at MRI, ICC volumes and sex.

comparison to FT infants. Furthermore, we show that the lower FA in most of these regions is due to a significantly increased RD, and no changes in AD. Indeed, maturational changes in anisotropy during development are predominantly attributable to a decrease in RD reflecting myelination and pre-myelination events, such as increased axonal calibre, decreased membrane permeability and development of functioning ionic channels (Partridge et al., 2004; Qiu et al., 2008; Suzuki et al., 2003; Wimberger et al., 1995). Since the regions with an increased RD in PTC vs FT infants are not myelinated at TEA, these increases cannot be attributed to myelin deficits per se, but could be due to a delayed or deficient wrapping of the oligodendrocytes around the axons before myelination, resulting in increased membrane permeability and a decreased axonal diameter, or to a greater spacing between axons constituting a WM fascicle (Counsell et al., 2006; Huppi et al., 1998). Our findings therefore confirm a decreased overall maturation of the WM in preterm control infants at TEA compared to the FT control group.

As for the PTM group, the mean FA, MD, RD and AD values, when averaging all the 20 ROI together, were not significantly different from FT newborns, suggesting overall similar maturity of the two groups. When evaluating mean diffusivities per ROI, mean FA was significantly reduced in PTM vs FT newborns only in "cc-sp", "cc-bd" and "fg-wm", regions where RD was increased. But, more importantly, in the "ec" region PTM had a higher mean FA compared to PTC infants. The small sample size might be hiding significant differences that are not evident in other regions, given these data. Indeed, other regions might be affected, as suggested by the tendency of PTM mean FA values to be superior to PTC and closer to FT infants in some of the regions, although we have not found a statistically significant difference.

The "ec" ROI comprises, due to our spatial resolution of 2x2x2mm^3, the external capsule, claustrum and extreme capsule. Through the extreme capsule pass bidirectional fibers providing communication between the claustrum and insular cortex, as well as between Broca's area

Table 5
Mean amygdala volumes corrected for GA at MRI, sex and ICC volumes and difference between groups.

	Amygdala Volumes (95% CI)			Statistical Results			
	Full-term	Preterm Music	Preterm Control	Group effect (p-value)	Pairwise comparison (p)		
					FT vs PTC	FT vs PTM	PTM vs PTC
Amygdala	514.9 (484.0–545.8)	492.2 (461.5–522.9)	422.9 (391.4–454.4)	**0.0001**	**0.001**	1	**0.006**
Left	521.3 (481.6–561.0)	496.4 (455.4–537.3)	422.4 (380.0–464.9)	0.665			
Right	508.4 (468.7–548.1)	488.0 (447.0–529.0)	423.4 (381.0–465.8)				

and Wernicke's area (Makris and Pandya, 2009). The insula is a multimodal area involved in music and emotion processing (Pouladi et al., 2010) and lesions in this area have been proven to alter emotional responses to music (Gosselin et al., 2005; Griffiths et al., 2004). Furthermore it is an integrant part of the salience network, which recently has been shown to present a decreased functional connectivity in PTC newborns in comparison to FT infants, but an enhanced functional connectivity in PTM (Lordier, 2019). The claustrum projects to and receives projections from several cortical areas, such as the auditory cortex, prefrontal cortex and cingulate cortex, as well as subcortical areas such as the hippocampus, amygdala and caudate nucleus (Amaral and Insausti, 1992; Crick and Koch, 2005) and has been shown to be involved in the processing of emotional faces in children (Pagliaccio et al., 2013). The external capsule is composed of claustro-cortical fibres dorsally, along with the combined mass of the uncinate fasciculus (connecting the amygdala to the OFC) and inferior frontal occipital fasciculus (IFOF) ventrally (connecting the occipital, posterior temporal and the orbito-frontal areas), and the anterior limb of the anterior commissure, which interconnects the amygdalae and the temporal lobes (Catani and Thiebaut de Schotten, 2008; Dejerine, 1985; Standring, 2015). Therefore, the improved structural maturation of this WM region provides evidence for a structural effect of the early preterm music intervention in these areas transited by WM fibers connecting areas involved in emotion and music processing.

4.2. Effects of prematurity and music on WM connectivity: tractography results

To deepen the study of the structural effect that the musical intervention could have on the VPT infants' brain, we performed tractography of two tracts involved in the processing of auditory information: the acoustic radiations, which relay the auditory information from the thalamus to primary auditory cortex; and the interhemispheric temporal callosal fibers, which transmit the auditory information between the two hemispheres.

Tractography analysis of acoustic radiations revealed, first, that the auditory thalamic route is structurally present already at TEA in both full-term and preterm infants, suggesting therefore that the sophisticated auditory behavior shown by infants early in life might well be cortical. Our findings are consistent with previous histochemical studies that have found evidence of thalamo-cortical afferents reaching the cortical plate after the 24th postconceptional week (Kostovic et al., 2002; Kostovic and Judas, 2010) and refute the model stating that the brainstem reticular-auditory pathway is the only existing path to the auditory cortex at birth (Eggermont and Moore, 2012). Second, analysis of acoustic radiations revealed that PTM presented a significantly higher mean FA than PTC group. In fact, training, including musical training, has been found to result in changes in WM microstructure measured by a higher FA, a finding that has been related to improved performance (Engel et al., 2014; Ruber et al., 2015; Taubert et al., 2012). Thus, our findings suggest an effect of the musical training in the maturation of acoustic radiations in preterm infants.

Regarding the interhemispheric temporal callosal fibers, our results suggest that PTC, who are exposed to an auditory environment very different from the mother's womb during early brain development, present a reduced maturation of these pathways at TEA, in comparison to FT newborns, as suggested by the reduced FA and increased MD, RD and AD. While the increased RD could be explained by possible deficits in premyelination, mean AD changes are more difficult to explain, but a decrease in mean AD has been reported in early development (Brouwer et al., 2012; Krogsrud et al., 2016; Mukherjee et al., 2002; Partridge et al., 2004; Qiu et al., 2008; Snook et al., 2005). A possible explanation for the diminished AD in early development might be related to the growth of neurofibrils, such as neurofilaments and microtubules, as well as glial cells during brain development, increasing axonal density or calibre, but also the tortuosity of extra-axonal space and diminishing the extra-axonal water content (Qiu et al., 2008; Takahashi et al., 2000). In contrast to the PTC, PTM presented an overall mean FA and AD closer to and not significantly different from FT newborns, again suggesting an improved WM tract maturation with the early activity induced by the music intervention.

We also performed tractography of the uncinate fasciculus, known to be implicated in socio-emotional processing and constituting the ventral part of the external capsule, which presented an increased FA in PTM vs PTC in our ROI-based analysis.

Tractography analysis of the uncinate fasciculus revealed that PTC had a decreased FA of this tract in comparison to FT newborns, while PTM presented a higher FA and diminished MD, RD and AD, suggesting an increased maturation of this tract after the music intervention.

Training, as well as experience during development, might influence myelination, promoted by neural firing across axons, and subsequently alter WM diffusion parameters (Demerens et al., 1996; Ishibashi et al., 2006; Zatorre et al., 2012), with typical diminished RD and increased FA – changes described after training in reading, working memory, music playing and meditation (Engvig et al., 2012; Hu et al., 2011; Keller and Just, 2009; Moore et al., 2017; Tang et al., 2012). Interestingly, it has been previously shown that musicians with absolute pitch ability have an increased FA in the uncinate fasciculus, in comparison to non-musicians.

The uncinate fasciculus is a WM association tract that connects parts of the limbic system in the temporal lobe, comprising the hippocampus and amygdala, with frontal regions, such as the OFC, which is involved in sensory integration and processing of affective stimuli (Kringelbach, 2005), evaluation of emotional association (Wildgruber et al., 2005) and top-down modulation of behavior (Ghashghaei and Barbas, 2002; Mcdonald, 1987). Neuroimaging studies of affective control in adults suggest prefrontal/orbitofrontal modulation of subcortical regions during emotion processing (Hariri et al., 2003; Keightley et al., 2003; Ochsner et al., 2002, 2004). Given the protracted development of the prefrontal cortex (Casey et al., 2000; Sowell et al., 1999), prefrontal-amygdala interactions are likely to play an important role in developmental changes in emotion processing. Connectivity analysis of 6 years-old infants born extremely preterm had revealed alterations in prefrontal cortico-basal ganglia-thalamocortical and limbic networks in these infants (Fischi-Gomez et al., 2016).

Our results suggest thus a decreased maturation of the uncinate fasciculus in PTC vs FT infants, in agreement with previous literature reporting a decreased FA in the uncinate fasciculus in adolescents (Constable et al., 2008; Mullen et al., 2011) and adults (Rimol et al., 2019) that were born prematurely. This finding may contribute to the behavioral socio-emotional difficulties present in prematurely born

infants later in development (Bhutta et al., 2002; Hille et al., 2001; Hughes et al., 2002; Lejeune et al., 2015; Montagna and Nosarti, 2016; Spittle et al., 2009; Witt et al., 2014). Multisensory stimulation as provided by the early music intervention in preterm infants might therefore induce specific WM tract maturation and improve brain connectivity in these networks, whose maturation was shown to be delayed in preterm newborns (Fischi-Gomez et al., 2015; Spittle et al., 2009) and which are key pathways for emotional processing (Koelsch, 2014).

4.3. Effects of prematurity and music on brain amygdala volume

The volumetric analysis of the brain amygdala showed that PTC infants, when at TEA, have a significantly smaller amygdala volume in comparison to FT infants, which is in agreement with the literature (Cismaru et al., 2016; Peterson et al., 2000).

It has been widely accepted that the amygdala, which is a primary structure of the brain limbic network, constitutes a central component of emotional processing and can regulate and modulate this network (Aggleton and Saunders, 2000). The amygdala processes emotions such as happiness, humour, anxiety, anger, fear and annoyance. It is involved in the assessment of emotional content of facial expressions and plays an important role in the recognition of and response to emotionally relevant social stimuli, thus participating in communication, social behavior and memory (Kraus and Canlon, 2012; Phan et al., 2002).

Studies on amygdala lesions in primates during the neonatal period have demonstrated exaggerated fear responses during social interactions (Bauman et al., 2004; Prather et al., 2001), which was interpreted as resulting from an incapacity to learn and recognize social cues that signal safety. Human studies have also suggested that amygdala lesions early in life dramatically impair processing of facial expressions (Adolphs et al., 1994, 1995).

Literature shows that premature newborns present an atypical socio-emotional development, comprising diminished social competences and self-esteem, emotional dysregulation, shyness and timidity (Bhutta et al., 2002; Hille et al., 2001; Hughes et al., 2002; Montagna and Nosarti, 2016; Spittle et al., 2009). In particular, VPT infants have been shown to present increased difficulties with regulating fear at 12 and 42-months-old (Langerock et al., 2013; Witt et al., 2014), as well as anger at 12 months (Langerock et al., 2013), frustration at 42 months accompanied by difficulties with decoding facial expressions of emotions (Witt et al., 2014), an immature sustained attention and inhibitory control at 24 months (Lejeune et al., 2015) and increased difficulties with recognizing emotional content and regulating social behavior at 5-7 years-old (Lejeune et al., 2016).

Biological and environmental factors associated with VPT birth are thus thought to lead to structural and functional alterations in brain areas involved in processing emotion and social stimuli. These alterations comprise, among others, a reduced amygdala volume (Cismaru et al., 2016; Peterson et al., 2000) and altered connectivity in prefrontal cortico-basal ganglia-thalamo-cortical and limbic networks (Fischi-Gomez et al., 2016; Witt et al., 2014).

Music has long been shown to be capable of evoking emotions (Ferguson and Sheldon, 2013; Lamont, 2011). Meta-interpretive literature reviews including functional neuroimaging studies have indicated that emotional stimuli, both negative and positive, are more likely to activate amygdala than neutral stimuli (Costafreda et al., 2008; Phan et al., 2002) and that the amygdala holds a central role in emotion modulation during music processing (Ball et al., 2007; Blood and Zatorre, 2001; Koelsch et al., 2013; Koelsch, 2014). Neuropsychological studies have further suggested that the amygdala is necessary in the emotional processing of music (Gosselin et al., 2005, 2007; Griffiths et al., 2004).

Our results show that VPT infants exposed to music during NICU stay, when at TEA, present a significantly larger amygdala volume in comparison to those receiving standard-of-care. This suggests that the music intervention in preterm infants might modulate amygdala activity during a critical period of brain development and thus have a structural impact on its volume. Since this region is part of a complex neural circuit, such modulation might also influence other brain regions within the circuitry, namely the orbitofrontal/prefrontal cortex, which is connected to the amygdala via the uncinate fasciculus, as suggested by our results on the improved microstructural maturation of this fasciculus by the music intervention. Together these brain structural effects might have an impact on VPT infants' later socio-emotional development. Indeed, preliminary clinical findings regarding the effect of this early postnatal music intervention on VPT infants' long-term emotional development revealed significantly decreased scores for fear-reactivity at 12 months and for anger-reactivity at 24 months' age in comparison to FT infants, with less important differences between PTM vs FT, than between PTC and FT newborns (Lejeune et al., 2019).

5. Conclusion

Overall brain microstructural maturation at TEA was decreased in VPT infants receiving the standard-of-care, when compared to FT newborns. Regions of significantly decreased maturation included the frontal white matter, genu, body and splenium of corpus callosum, anterior commissure, fornix minor, posterior limb of internal capsule, inferior longitudinal fasciculus, medial temporal gyrus white matter, external capsule/claustrum/extreme capsule, interhemispherical auditory callosal fibers and uncinate fasciculus.

VPT infants listening to music during NICU stay, in comparison to VPT infants receiving the standard-of-care, showed an increased WM microstructural maturation in acoustic radiations, external capsule/claustrum/extreme capsule and uncinate fasciculus, as well as larger amygdala volumes, all of which are brain structures involved in acoustic and/or emotion processing.

This is the first neuroimaging clinical study showing a structural impact of a music intervention created specifically for premature infants upon the maturation of brain regions known to be altered by prematurity and which hold key roles in emotional processing. In particular, the effect of music on the amygdala volume and on the maturation of the uncinate fasciculus, described by using two independent MRI techniques, supports the clinical use of such an intervention in mitigating later social-emotional difficulties associated with prematurity.

Limitations, technical considerations and future directions

One limitation of the study is the modest sample size for a randomized clinical trial and the limited number of times of music exposition.

The modest sample size and the specificity of our neonatal population imposes some technical considerations. For an overall evaluation of the impact of the intervention in the main WM tracts, we opted for a template-based region-of-interest (ROI) analysis method comprising 20 different WM ROI. Due to the diffusion imaging resolution (2x2x2 mm^3), this technique may be affected by the partial volume problem. However, automated whole-brain diffusion-based group analysis techniques such as TBSS and TSA were considered less suited to our study, since they are generally appropriate for larger cohorts and have been proven to be less suitable to neonatal population (Pecheva et al., 2017). In particular, robust medial tracts are difficult to compute from the premature infant's thin sheet-like tracts, making TSA less appropriate to study certain WM fibers of interest to our hypothesis.

We would also like to point out that mean DTI metrics, such as mean FA, depend on the number of crossings and microstructural complexity, which varies with age. For this reason, we have scanned our population within at a narrow age range and we have controlled the data for the infant's age at the MRI.

Despite the relatively limited number of times of music exposition, our intervention results are encouraging. Thus, currently we are replicating this music intervention study on a second population in order to assess the reproducibility of the music effect. We have further increased the number of music expositions per day and included an MRI before, in

addition to the one after the intervention, to decrease inter-subject variability bias, using a multi-shell diffusion protocol.

This study compared instrumental music intervention to standard-of-care in the NICU. We show that this early intervention in preterm newborns leads to an increased structural brain maturation specifically of some auditory and emotional processing pathways. However, parental presence and exposure to speech (namely maternal singing), considered to be equally distributed between groups given the process of random allocation, were not individually quantified and might also have an impact in infant's brain development. More research is needed to compare this instrumental music intervention to other sound interventions such as maternal singing.

The clinical significance of these brain structural effects of music remains to be evaluated by investigating neurodevelopmental and cognitive outcomes in childhood planned for future follow-up studies.

Funding

This study was supported by the Swiss National Science Foundation n°32473B_135817/1, n° 324730-163084 and Prim'enfance foundation.

Author contributions section

Joana Sa de Almeida: Formal analysis, Software, Conceptualization, Writing-Original Draft; **Lara Lordier:** Investigation, Writing-Review & Editing; **Benjamin Zollinger:** Formal analysis, Writing-Review & Editing; **Nicolas Kunz**: Methodology, Software; **Matteo Bastiani:** Methodology, Software, Formal analysis, Writing-Review & Editing; **Laura Gui:** Formal analysis, Writing-Review & Editing; **Alexandra Adam-Darque:** Investigation; **Cristina Borradori-Tolsa**: Writing-Review & Editing; **François Lazeyras:** Resources, Investigation; **Petra S. Hüppi:** Conceptualization, Writing-Review&Editing, Supervision, Project administration, Resources, Funding acquisition.

Declaration of competing interest

The authors declare no competing interests.

Acknowledgments

The authors thank all clinical staff, namely in neonatology and unit of development of HUG Pediatric Hospital, all parents and newborns participating in the project, the Pediatrics Clinic Research Platform and the Center for Biomedical Imaging (CIBM) of the University Hospitals of Geneva, for all their help and support. Special acknowledgment to Dr. Samuel Sommaruga, MD-PhD, neurosurgeon with expertise in neuroanatomy, for his contribution to amygdala segmentation correction.

Appendix A. Supplementary data

Supplementary data to this article can be found online at https://doi.org/10.1016/j.neuroimage.2019.116391.

References

Aanes, S., et al., 2015. Memory function and hippocampal volumes in preterm born very-low-birth-weight (VLBW) young adults. Neuroimage 105, 76–83.
Adibpour, P., Dubois, J., Dehaene-Lambertz, G., 2018. Right but not left hemispheric discrimination of faces in infancy. Nat. Hum. Behav. 2, 67–79.
Adolphs, R., et al., 1994. Impaired recognition of emotion in facial expressions following bilateral damage to the human amygdala. Nature 372, 669–672.
Adolphs, R., et al., 1995. Fear and the human amygdala. J. Neurosci. 15, 5879–5891.
Aeby, A., et al., 2009. Maturation of thalamic radiations between 34 and 41 weeks' gestation: a combined voxel-based study and probabilistic tractography with diffusion tensor imaging. AJNR Am J Neuroradiol 30, 1780–1786.
Aggleton, J.P., Saunders, C., 2000. The amygdala - what's happened in the last decade. In: The Amygdala: a Functional Analysis. Oxford University Press, Oxford, pp. 1–30.
Akazawa, K., et al., 2016. Probabilistic maps of the white matter tracts with known associated functions on the neonatal brain atlas: application to evaluate longitudinal developmental trajectories in term-born and preterm-born infants. Neuroimage 128, 167–179.
Als, H., McAnulty, G., 2014. The Newborn Individualized Developmental Care and Assessment Program (NIDCAP) with Kangaroo Mother Care (KMC): Comprehensive Care for Preterm Infants.
Amaral, D.G., Insausti, R., 1992. Retrograde transport of D-[H-3]-Aspartate injected into the monkey amygdaloid complex. Exp. Brain Res. 88, 375–388.
Anderson, P., Doyle, L.W., 2003. Neurobehavioral outcomes of school-age children born extremely low birth weight or very preterm in the 1990s. JAMA, J. Am. Med. Assoc. 289, 3264–3272.
Andersson, J.L.R., et al., 2016. Incorporating outlier detection and replacement into a non-parametric framework for movement and distortion correction of diffusion MR images. Neuroimage 141, 556–572.
Andersson, J.L.R., Sotiropoulos, S.N., 2016. An integrated approach to correction for off-resonance effects and subject movement in diffusion MR imaging. Neuroimage 125, 1063–1078.
Andersson, J.L.R., et al., 2017. Towards a comprehensive framework for movement and distortion correction of diffusion MR images: within volume movement. Neuroimage 152, 450–466.
Anjari, M., et al., 2007. Diffusion tensor imaging with tract-based spatial statistics reveals local white matter abnormalities in preterm infants. Neuroimage 35, 1021–1027.
Arpi, E., Ferrari, F., 2013. Preterm birth and behaviour problems in infants and preschool-age children: a review of the recent literature. Dev. Med. Child Neurol. 55, 788–796.
Ball, G., et al., 2012. The effect of preterm birth on thalamic and cortical development. Cerebr. Cortex 22, 1016–1024.
Ball, G., et al., 2017. Multimodal image analysis of clinical influences on preterm brain development. Ann. Neurol. 82, 233–246.
Ball, T., et al., 2007. Response properties of human amygdala subregions: evidence based on functional MRI combined with probabilistic anatomical maps. PLoS One 2.
Bassi, L., et al., 2008. Probabilistic diffusion tractography of the optic radiations and visual function in preterm infants at term equivalent age. Brain 131, 573–582.
Bastiani, M., et al., 2019. Automated processing pipeline for neonatal diffusion MRI in the developing Human Connectome Project. Neuroimage 185, 750–763.
Bauman, M.D., et al., 2004. The development of social behavior following neonatal amygdala lesions in rhesus monkeys. J. Cogn. Neurosci. 16, 1388–1411.
Beaulieu, C., 2002. The basis of anisotropic water diffusion in the nervous system - a technical review. NMR Biomed. 15, 435–455.
Behrens, T.E.J., et al., 2003. Characterization and propagation of uncertainty in diffusion-weighted MR imaging. Magn. Reson. Med. 50, 1077–1088.
Behrens, T.E.J., et al., 2007. Probabilistic diffusion tractography with multiple fibre orientations: what can we gain? Neuroimage 34, 144–155.
Bhutta, A.T., et al., 2002. Cognitive and behavioral outcomes of school-aged children who were born preterm - a meta-analysis. JAMA, J. Am. Med. Assoc. 288, 728–737.
Blencowe, H., et al., 2013. Born too soon: the global epidemiology of 15 million preterm births. Reprod. Health 10 (Suppl. 1). S2-S2.
Blood, A.J., Zatorre, R.J., 2001. Intensely pleasurable responses to music correlate with activity in brain regions implicated in reward and emotion. Proc. Natl. Acad. Sci. U. S. A. 98, 11818–11823.
Brody, B.A., et al., 1987. Sequence of central nervous system myelination in human infancy. I. An autopsy study of myelination. J. Neuropathol. Exp. Neurol. 46, 283–301.
Brouwer, R.M., et al., 2012. White matter development in early puberty: a longitudinal volumetric and diffusion tensor imaging twin study. PLoS One 7.
Casey, B.J., Giedd, J.N., Thomas, K.M., 2000. Structural and functional brain development and its relation to cognitive development. Biol. Psychol. 54, 241–257.
Catani, M., Thiebaut de Schotten, M., 2008. A diffusion tensor imaging tractography atlas for virtual in vivo dissections. Cortex. J. Devoted Study. Nerv. Syst. Behav. 44, 1105–1132.
Chang, E., 2015. Preterm birth and the role of neuroprotection. BMJ Br. Med. J. (Clin. Res. Ed.) 350.
Cismaru, A.L., et al., 2016. Altered amygdala development and fear processing in prematurely born infants. Front. Neuroanat. 10, 55.
Constable, R.T., et al., 2008. Prematurely born children demonstrate white matter microstructural differences at 12 years of age, relative to term control subjects: an investigation of group and gender effects. Pediatrics 121, 306–316.
Costafreda, S.G., et al., 2008. Predictors of amygdala activation during the processing of emotional stimuli: a meta-analysis of 385 PET and fMRI studies. Brain Res. Rev. 58, 57–70.
Counsell, S.J., et al., 2006. Axial and radial diffusivity in preterm infants who have diffuse white matter changes on magnetic resonance imaging at term-equivalent age. Pediatrics 117, 376–386.
Counsell, S.J., et al., 2008. Specific relations between neurodevelopmental abilities and white matter microstructure in children born preterm. Brain 131, 3201–3208.
Crick, F.C., Koch, C., 2005. What is the function of the claustrum? Philos. Trans. R. Soc. Biol. Sci. 360, 1271–1279.
Dejerine, J., 1985. Classics in neurology - intermittent claudication of the spinal-cord (reprinted from semiologie des affections du systeme nerveux, P9 267-269, 1914). Neurology 35, 860-860.
Demerens, C., et al., 1996. Induction of myelination in the central nervous system by electrical activity. Proc. Natl. Acad. Sci. U.S.A. 93, 9887–9892.
Dubois, J., et al., 2008. Asynchrony of the early maturation of white matter bundles in healthy infants: quantitative landmarks revealed noninvasively by diffusion tensor imaging. Hum. Brain Mapp. 29, 14–27.
Duerden, E.G., et al., 2015. Tract-based spatial statistics in preterm-born neonates predicts cognitive and motor outcomes at 18 months. Am. J. Neuroradiol. 36, 1565–1571.

Dyet, L.E., et al., 2006. Natural history of brain lesions in extremely preterm infants studied with serial magnetic resonance imaging from birth and neurodevelopmental assessment. Pediatrics 118, 536–548.
Eggermont, J.J., Moore, J.K., 2012. Morphological and functional development of the auditory nervous system. In: Werner, L.a.F., Richard, R., Popper, Arthur N. (Eds.), Human Auditory Development, pp. 61–105.
Engel, A., et al., 2014. Inter-individual differences in audio-motor learning of piano melodies and white matter fiber tract architecture. Hum. Brain Mapp. 35, 2483–2497.
Engvig, A., et al., 2012. Memory training impacts short-term changes in aging white matter: a Longitudinal Diffusion Tensor Imaging Study. Hum. Brain Mapp. 33, 2390–2406.
Ferguson, Y.L., Sheldon, K.M., 2013. Trying to be happier really can work: two experimental studies. J. Posit. Psychol. 8, 23–33.
Fischi-Gomez, E., et al., 2015. Structural brain connectivity in school-age preterm infants provides evidence for impaired networks relevant for higher order cognitive skills and social cognition. Cerebr. Cortex 25, 2793–2805.
Fischi-Gomez, E., et al., 2016. Brain network characterization of high-risk preterm-born school-age children. Neuroimage: Clinica 11, 195–209.
Ghashghaei, H.T., Barbas, H., 2002. Pathways for emotion: interactions of prefrontal and anterior temporal pathways in the amygdala of the rhesus monkey. Neuroscience 115, 1261–1279.
Gimenez, M., et al., 2006. Abnormal orbitofrontal development due to prematurity. Neurology 67, 1818–1822.
Gosselin, N., et al., 2005. Impaired recognition of scary music following unilateral temporal lobe excision. Brain 128, 628–640.
Gosselin, N., et al., 2007. Amygdala damage impairs emotion recognition from music. Neuropsychologia 45, 236–244.
Gousias, I.S., et al., 2012. Magnetic resonance imaging of the newborn brain: manual segmentation of labelled atlases in term-born and preterm infants. Neuroimage 62, 1499–1509.
Graven, S.N., Browne, J.V., 2008. Auditory development in the fetus and infant. N.born Infant Nurs. Rev. 8, 187–193.
Griffiths, T.D., et al., 2004. When the feeling's gone": a selective loss of musical emotion. J. Neurol. Neurosurg. Psychiatry 75, 344–345.
Groppo, M., et al., 2014. Development of the optic radiations and visual function after premature birth. Cortex 56, 30–37.
Gui, L., et al., 2012. Morphology-driven automatic segmentation of MR images of the neonatal brain. Med. Image Anal. 16, 1565–1579.
Hariri, A.R., et al., 2003. Neocortical modulation of the amygdala response to fearful stimuli. Biol. Psychiatry 53, 494–501.
Hille, E.T.M., et al., 2001. Behavioural problems in children who weigh 1000 g or less at birth in four countries. Lancet 357, 1641–1643.
Hu, Y.Z., et al., 2011. Enhanced white matter tracts integrity in children with abacus training. Hum. Brain Mapp. 32, 10–21.
Huang, H., et al., 2006. White and gray matter development in human fetal, newborn and pediatric brains. Neuroimage 33, 27–38.
Hughes, M.B., et al., 2002. Temperament characteristics of premature infants in the first year of life. J. Dev. Behav. Pediatr. 23, 430–435.
Huppi, P.S., et al., 1998. Microstructural development of human newborn cerebral white matter assessed in vivo by diffusion tensor magnetic resonance imaging. Pediatr. Res. 44, 584–590.
Huppi, P.S., Dubois, J., 2006. Diffusion tensor imaging of brain development. Semin. Fetal Neonatal Med. 11, 489–497.
Inder, T.E., et al., 2005. Abnormal cerebral structure is present at term in premature infants. Pediatrics 115, 286–294.
Ishibashi, T., et al., 2006. Astrocytes promote myelination in response to electrical impulses. Neuron 49, 823–832.
Johnson, S., Marlow, N., 2011. Preterm birth and childhood psychiatric disorders. Pediatr. Res. 69, 11R-8R.
Jones, D.K., 2011. Diffusion MRI — Theory, Methods and Applications. Oxford University Press USA, New York.
Kamagata, K., et al., 2012. White matter alteration of the cingulum in Parkinson disease with and without dementia: evaluation by diffusion tensor tract-specific analysis. Am. J. Neuroradiol. 33, 890–895.
Keightley, M.L., et al., 2003. An fMRI study investigating cognitive modulation of brain regions associated with emotional processing of visual stimuli. Neuropsychologia 41, 585–596.
Keller, T.A., Just, M.A., 2009. Altering cortical connectivity: remediation-induced changes in the white matter of poor readers. Neuron 64, 624–631.
Kiss, J.Z., Vasung, L., Petrenko, V., 2014. Process of cortical network formation and impact of early brain damage. Curr. Opin. Neurol. 27, 133–141.
Kochunov, P., et al., 2009. Analysis of genetic variability and whole genome linkage of whole-brain, subcortical, and ependymal hyperintense white matter volume. Stroke 40, 3685–3690.
Koelsch, S., et al., 2004. Music, language and meaning: brain signatures of semantic processing. Nat. Neurosci. 7, 302–307.
Koelsch, S., 2010. Towards a neural basis of music-evoked emotions. Trends Cogn. Sci. 14, 131–137.
Koelsch, S., et al., 2013. The roles of superficial amygdala and auditory cortex in music-evoked fear and joy. Neuroimage 81, 49–60.
Koelsch, S., 2014. Brain correlates of music-evoked emotions. Nat. Rev. Neurosci. 15, 170–180.
Kostovic, I., et al., 2002. Laminar organization of the human fetal cerebrum revealed by histochemical markers and magnetic resonance imaging. Cerebr. Cortex 12, 536–544.
Kostovic, I., Judas, M., 2010. The development of the subplate and thalamocortical connections in the human foetal brain. Acta Paediatr. 99, 1119–1127. Oslo, Norway : 1992.
Kraus, K.S., Canlon, B., 2012. Neuronal connectivity and interactions between the auditory and limbic systems. Effects of noise and tinnitus. Hear. Res. 288, 34–46.
Kringelbach, M.L., 2005. The human orbitofrontal cortex: linking reward to hedonic experience. Nat. Rev. Neurosci. 6, 691–702.
Krishnan, M.L., et al., 2007. Relationship between white matter apparent diffusion coefficients in preterm infants at term-equivalent age and developmental outcome at 2 years. Pediatrics 120, E604–E609.
Krogsrud, S.K., et al., 2016. Changes in white matter microstructure in the developing brain-A longitudinal diffusion tensor imaging study of children from 4 to 11 years of age. Neuroimage 124, 473–486.
Lamont, A., 2011. University students' strong experiences of music: pleasure, engagement, and meaning. Music. Sci. 15, 229–249.
Langerock, N., et al., 2013. Emotional reactivity at 12 months in very preterm infants born at <29 weeks of gestation. Infant Behav. Dev. 36, 289–297.
Largo, R., et al., 1989. Significance of prenatal, perinatal and postnatal factors in the development of AGA preterm infants at five to seven years. Dev. Med. Child Neurol. 31, 440–456.
Lasky, R.E., Williams, A.L., 2005. The development of the auditory system from conception to term. NeoReviews 6, e141–e152.
Lejeune, F., et al., 2015. Emotion, attention, and effortful control in 24-month-old very preterm and full-term children. Année Psychol. 115, 241–264.
Lejeune, F., et al., 2016. Social reasoning abilities in preterm and full-term children aged 5-7years. Early Hum. Dev. 103, 49–54.
Lejeune, F., et al., 2019. Effects of an early postnatal music intervention on cognitive and emotional development in preterm children at 12 and 24 Months: preliminary findings. Front. Psychol. 10, 494.
Loe, I.M., Lee, E.S., Feldman, H.M., 2013. Attention and internalizing behaviors in relation to white matter in children born preterm. J. Dev. Behav. Pediatr. 34, 156–164.
Lordier, L., et al., 2019b. Music in premature infants enhances high-level cognitive brain networks. Proc. Natl. Acad. Sci. U.S.A. 116, 12103–12108.
Lordier, L., et al., 2019a. Music processing in preterm and full-term newborns: a psychophysiological interaction (PPI) approach in neonatal fMRI. Neuroimage 185, 857–864.
Makris, N., Pandya, D.N., 2009. The extreme capsule in humans and rethinking of the language circuitry. Brain Struct. Funct. 213, 343–358.
Marlow, N., 2004. Neurocognitive outcome after very preterm birth. Arch. Dis. Child. Fetal Neonatal Ed. 89, F224–F228.
Mcdonald, A.J., 1987. Somatostatinergic projections from the amygdala to the bed nucleus of the stria terminalis and medial preoptic-hypothalamic region. Neurosci. Lett. 75, 271–277.
Ment, L.R., Hirtz, D., Huppi, P.S., 2009. Imaging biomarkers of outcome in the developing preterm brain. Lancet Neurol. 8, 1042–1055.
Montagna, A., Nosarti, C., 2016. Socio-emotional development following very preterm birth: pathways to psychopathology. Front. Psychol. 7.
Moore, E., et al., 2017. Diffusion tensor MRI tractography reveals increased fractional anisotropy (FA) in arcuate fasciculus following music-cued motor training. Brain Cogn. 116, 40–46.
Mukherjee, P., et al., 2002. Diffusion-tensor MR imaging of gray and white matter development during normal human brain maturation. AJNR Am J Neuroradiol 23, 1445–1456.
Mullen, K.M., et al., 2011. Preterm birth results in alterations in neural connectivity at age 16 years. Neuroimage 54, 2563–2570.
Neil, J., et al., 2002. Diffusion tensor imaging of normal and injured developing human brain - a technical review. NMR Biomed. 15, 543–552.
Nosarti, C., et al., 2012. Preterm birth and psychiatric disorders in young adult life. Arch. Gen. Psychiatr. 69, 610–617.
Nosarti, C., 2013. Structural and functional brain correlates of behavioral outcomes during adolescence. Early Hum. Dev. 89, 221–227.
Nosarti, C., et al., 2014. Preterm birth and structural brain alterations in early adulthood. Neuroimage-Clinical. 6, 180–191.
Nossin-Manor, R., et al., 2013. Quantitative MRI in the very preterm brain: assessing tissue organization and myelination using magnetization transfer, diffusion tensor and T-1 imaging. Neuroimage 64, 505–516.
Ochsner, K.N., et al., 2002. Rethinking feelings: an fMRI study of the cognitive regulation of emotion. J. Cogn. Neurosci. 14, 1215–1229.
Ochsner, K.N., et al., 2004. For better or for worse: neural systems supporting the cognitive down- and up-regulation of negative emotion. Neuroimage 23, 483–499.
Oishi, K., et al., 2010. MRI Atlas of Human White Matter. Academic Press.
Onu, M., et al., 2012. Diffusion abnormality maps in demyelinating disease: correlations with clinical scores. Eur. J. Radiol. 81, E386–E391.
Padilla, N., et al., 2015. Brain Growth Gains and Losses in Extremely Preterm Infants at Term. Cerebral Cortex, vol.25, pp. 1897–1905. New York, N.Y. : 1991.
Pagliaccio, D., et al., 2013. Functional brain activation to emotional and nonemotional faces in healthy children: evidence for developmentally undifferentiated amygdala function during the school-age period. Cognit. Affect Behav. Neurosci. 13, 771–789.
Partridge, S.C., et al., 2004. Diffusion tensor imaging: serial quantitation of white matter tract maturity in premature newborns. Neuroimage 22, 1302–1314.
Pecheva, D., et al., 2017. A tract-specific approach to assessing white matter in preterm infants. Neuroimage 157, 675–694.
Pecheva, D., et al., 2018. Recent Advances in Diffusion Neuroimaging: Applications in the Developing Preterm Brain, vol. 7. F1000Res.

Perani, D., et al., 2010. Functional specializations for music processing in the human newborn brain. Proc. Natl. Acad. Sci. U.S.A. 107, 4758–4763.
Peterson, B.S., et al., 2000. Regional brain volume abnormalities and long-term cognitive outcome in preterm infants. JAMA, J. Am. Med. Assoc. 284, 1939–1947.
Phan, K.L., et al., 2002. Functional neuroanatomy of emotion: a meta-analysis of emotion activation studies in PET and fMRI. Neuroimage 16, 331–348.
Pierpaoli, C., Basser, P.J., 1996. Toward a quantitative assessment of diffusion anisotropy. Magn. Reson. Med. 36, 893–906.
Popescu, M., Otsuka, A., Ioannides, A.A., 2004. Dynamics of brain activity in motor and frontal cortical areas during music listening: a magnetoencephalographic study. Neuroimage 21, 1622–1638.
Pouladi, F., et al., 2010. Involved brain areas in processing of Persian classical music: an fMRI study. Procedia. Soc. Behav. Sci. 5, 1124–1128.
Prather, M.D., et al., 2001. Increased social fear and decreased fear of objects in monkeys with neonatal amygdala lesions. Neuroscience 106, 653–658.
Qiu, D.Q., et al., 2008. Diffusion tensor imaging of normal white matter maturation from late childhood to young adulthood: voxel-wise evaluation of mean diffusivity, fractional anisotropy, radial and axial diffusivities, and correlation with reading development. Neuroimage 41, 223–232.
Radley, J.J., Morrison, J.H., 2005. Repeated stress and structural plasticity in the brain. Ageing Res. Rev. 4, 271–287.
Rimol, L.M., et al., 2019. Reduced white matter fractional anisotropy mediates cortical thickening in adults born preterm with very low birthweight. Neuroimage 188, 217–227.
Rogers, C.E., et al., 2012. Regional cerebral development at term relates to school-age social-emotional development in very preterm children. J. Am. Acad. Child Adolesc. Psychiatry 51, 181–191.
Rose, S.E., et al., 2008. Altered white matter diffusion anisotropy in normal and preterm infants at term-equivalent age. Magn. Reson. Med. 60, 761–767.
Ruber, T., Lindenberg, R., Schlaug, G., 2015. Differential adaptation of descending motor tracts in musicians. Cerebr. Cortex 25, 1490–1498.
Shim, S.Y., et al., 2012. Altered microstructure of white matter except the corpus callosum is independent of prematurity. Neonatology 102, 309–315.
Sizun, J., Westrup, B., 2004. Early developmental care for preterm neonates: a call for more research. Arch. Dis. Child. Fetal Neonatal Ed. 89, F384–F388.
Skranes, J., et al., 2007. Clinical findings and white matter abnormalities seen on diffusion tensor imaging in adolescents with very low birth weight. Brain 130, 654–666.
Smith, S.M., et al., 2004. Advances in functional and structural MR image analysis and implementation as FSL. Neuroimage 23, S208–S219.
Snook, L., et al., 2005. Diffusion tensor imaging of neuro development in children and young adults. Neuroimage 26, 1164–1173.
Sowell, E.R., et al., 1999. In vivo evidence for post-adolescent brain maturation in frontal and striatal regions. Nat. Neurosci. 2, 859–861.
Spittle, A.J., et al., 2009. Early emergence of behavior and social-emotional problems in very preterm infants. J. Am. Acad. Child Adolesc. Psychiatry 48, 909–918.
Spittle, A.J., et al., 2011. Neonatal white matter abnormality predicts childhood motor impairment in very preterm children. Dev. Med. Child Neurol. 53, 1000–1006.
Standring, S., 2015. Gray's Anatomy: the Anatomical Basis of Clinical Practice. Elsevier, Edinburgh: Churchill Livingstone.
Suzuki, Y., et al., 2003. Absolute eigenvalue diffusion tensor analysis for human brain maturation. NMR Biomed. 16, 257–260.
Takahashi, M., et al., 2000. Diffusional anisotropy in cranial nerves with maturation: quantitative evaluation with diffusion MR imaging in rats. Radiology 216, 881–885.
Tang, Y.Y., et al., 2012. Mechanisms of white matter changes induced by meditation. Proc. Natl. Acad. Sci. U.S.A. 109, 10570–10574.
Taubert, M., Villringer, A., Ragert, P., 2012. Learning-related gray and white matter changes in humans: an update. The Neuroscientist 18, 320–325.
Thompson, D.K., et al., 2007. Perinatal risk factors altering regional brain structure in the preterm infant. Brain 130, 667–677.
Thompson, D.K., et al., 2011. Characterization of the corpus callosum in very preterm and full-term infants utilizing MRI. Neuroimage 55, 479–490.
Thompson, D.K., et al., 2013. Hippocampal shape variations at term equivalent age in very preterm infants compared with term controls: perinatal predictors and functional significance at age 7. Neuroimage 70, 278–287.
Treyvaud, K., et al., 2013. Psychiatric outcomes at age seven for very preterm children: rates and predictors. JCPP (J. Child Psychol. Psychiatry) 54, 772–779.
Volpe, J.J., 2009. The encephalopathy of prematurity–brain injury and impaired brain development inextricably intertwined. Semin. Pediatr. Neurol. 16, 167–178.
Webb, A.R., et al., 2015. Mother's voice and heartbeat sounds elicit auditory plasticity in the human brain before full gestation. Proc. Natl. Acad. Sci. U.S.A. 112, 3152–3157.
Wildgruber, D., et al., 2005. Identification of emotional intonation evaluated by fMRI. Neuroimage 24, 1233–1241.
Williams, J., Lee, K.J., Anderson, P.J., 2010. Prevalence of motor-skill impairment in preterm children who do not develop cerebral palsy: a systematic review. Dev. Med. Child Neurol. 52, 232–237.
Wimberger, D.M., et al., 1995. Identification of "premyelination" by diffusion-weighted MRI. J. Comput. Assist. Tomogr. 19, 28–33.
Witt, A., et al., 2014. Emotional and effortful control abilities in 42-month-old very preterm and full-term children. Early Hum. Dev. 90, 565–569.
Yushkevich, P.A., et al., 2006. User-guided 3D active contour segmentation of anatomical structures: significantly improved efficiency and reliability. Neuroimage 31, 1116–1128.
Zatorre, R.J., Peretz, I., Penhune, V., 2009. Neuroscience and music ("Neuromusic") III: disorders and plasticity. Ann. N. Y. Acad. Sci. 1169, 1–2.
Zatorre, R.J., Fields, R.D., Johansen-Berg, H., 2012. Plasticity in gray and white: neuroimaging changes in brain structure during learning. Nat. Neurosci. 15, 528–536.
Zhang, H., et al., 2006. Deformable registration of diffusion tensor MR images with explicit orientation optimization. Med. Image Anal. 10, 764–785.